the longer transcript encoded a new variant containing 48 extra nucleotides at the 5' end (Figure 1a). We named the novel longer transcript Siah-1L. To clarify which Siah-1 transcript was actually induced by p53, we further investigated the expression of human Siah-1 transcripts in MCF7 cells after treatment with doxorubicin (DOX; Calbiochem, San Diego, CA, USA), which is known to induce p53 activation. As shown in Figure 1b, an endogenous 897-bp Siah-1L transcript was barely detectable in control cells; however, the expression of Siah-1L mRNA was strongly induced 6–12 h after DOX treatment (Figure 1b, upper panel). In contrast, the 849-bp Siah-1 mRNA remained unchanged (Figure 1b, middle panel). The increase in Siah-1L mRNA levels prompted us to examine whether the protein levels changed in response to DOX treatment. Next, we analysed the expression levels of p53, β-catenin, and Siah-1-family proteins. As shown in Figure 1c, p53 protein expression was strongly induced 6 h after treatment with DOX and the expression peaked at 12 h. The level of endogenous β-catenin protein started to decrease 24 h and showed a marked reduction 36 h after treatment. The expression of endogenous Siah-1-family proteins was low in control cells; however, Siah-1L but not Siah-1 was upregulated 12 h after DOX treatment (Figure 1c, lower panel).

To further investigate whether Siah-1L was induced in a p53-dependent manner, we examined the expression levels of Siah-family proteins and β-catenin in cells after UV irradiation. As shown in Figure 1d, the Siah-1L transcript increased 12 h after UV irradiation in MCF7 cells; in contrast, UV treatment did not trigger any changes in the level of Siah-1 transcript. Furthermore, Siah-1L protein expression was markedly increased in response to UV treatment, and the elevation of p53 protein and the degradation of β-catenin were also observed at the same time (Figure 1e).

Next, we investigated the expression levels of Siah-1L transcript in Hep3B cells, which have been reported to lack both copies of the p53 gene (Lee et al., 2002). Expression of the p53 and β-catenin proteins was analysed by Western blots after DOX treatment. As expected, the p53 protein was undetectable in lysates derived from control cells and DOX-treated cells (Figure 1f). The expression of endogenous β-catenin protein did not change in the presence of DOX (Figure 1f). The Siah-1 transcript was detectable in control cells and was not changed when the cells were treated with DOX (Figure 1g, middle panel). In contrast, the Siah-1L mRNA was undetectable in the presence and absence of DOX (Figure 1g, upper panel). These findings further suggest that Siah-1L is upregulated in response to p53 activity.

To determine whether the induction of Siah-1L expression is specifically dependent on p53, MCF7 and Hep3B cells were transiently transfected with expression plasmids encoding wild-type or mutant p53, and Siah-1-family transcripts were analysed by RT–PCR. As shown in Figure 2a, increased amounts of Siah-1L mRNA were found in p53-expressing MCF7 cells, but not in control cells. Siah-1 mRNA remained unchanged in cells after

the overexpression of p53 protein. Mutant p53 did not upregulate the Siah-1L mRNA, and instead decreased its expression (Figure 2a). To explore the role of Siah-1L in the regulation of β-catenin activity, we analysed the expression of β-catenin protein in cells transfected with wild-type or mutant p53. Levels of β-catenin protein were significantly lower in p53-overexpressing cells compared with both control and p53-mutant-expressing cells (Figure 2b). Since loss of p53 function is a frequent event in various human cancer cells, we then tested whether Siah-1L could be induced by exogenous p53 in cells that lack functional p53. As shown in Figure 2c, Siah-1L mRNA was significantly upregulated in p53-expressing Hep3B cells, while Siah-1L transcript was undetectable in control and mutant p53-expressing cells. The expression levels of Siah-1 were unchanged in p53-expressing cells compared to control cells (Figure 2c). Notably, levels of β-catenin protein were markedly decreased in endogenous p53-deficient cells after transfection with the p53 expression plasmid (Figure 2d). Next, to clarify whether Siah-1L is responsible for the p53-mediated degradation of β-catenin, we employed the short interfering RNA (siRNA) approach and used an expression plasmid encoding Siah-1 lacking the RING finger domain (pcDNA3-FLAG-Siah-1ΔRING), which is a dominant-negative form of Siah-1L. We showed the siRNA specific for Siah-1L (siSiah-1L) induced the reduction of the transfected Siah-1L, not Siah-1, in HEK293T cells (Figure 2e). In contrast, control siRNA (siCTR) did not show any effect of the protein levels of Siah-1L and Siah-1. Moreover, in the p53-transfected cells, siSiah-1L markedly reduced the expression level of endogenous Siah-1L, but not Siah-1 transcript (Figure 2f). To examine the protein levels of β-catenin in the Siah-1L knockdown cells, we performed Western blots. Transfection of siSiah-1L had almost rescued the p53-induced degradation of β-catenin (Figure 2g). However, this recovery of the β-catenin protein levels was not observed in siCTR-transfected cells. We also demonstrated that the protein levels of β-catenin were recovered in the cells cotransfected with expression plasmids encoding FLAG-Siah-1ΔRING and p53 from the p53-dependent degradation (Figure 2h). Taken together, these findings suggest that p53 specifically enhances the expression of Siah-1L and is involved in the regulation of β-catenin protein degradation via the expression of Siah-1L.

Siah-1L suppresses Tcf/LEF transcriptional activity and enhances the degradation of β-catenin

To explore the functional significance of p53-inducible Siah-1L expression, we asked whether Siah-1L production affects β-catenin activity in cells. Since β-catenin forms a complex with a member of the T-cell factor (Tcf)/lymphocyte enhancer-binding factor (LEF) family and activated the target genes (Omer et al., 1999), reporter assays were performed to monitor Tcf/LEF-dependent gene expression in the presence or absence of Siah-1L or Siah-1. We used pcDNA3-FLAG-Siah-1ΔRING, which is a dominant-negative form of

Siah-1L, as a negative control. In addition, a reporter plasmid with a mutated Tcf-binding site was also used as a negative control for the reporter assay. As shown in Figure 3a, about a 40-fold augmentation of relative luciferase activity was found in cells transfected with an expression plasmid encoding β-catenin. When Siah-1L was produced in cells, the level of Tcf/LEF transcriptional activity induced by overexpression of β-catenin was markedly decreased compared with that in control cells (Figure 3a). In contrast, a plasmid encoding Siah-1ΔRING did not decrease reporter activity, instead slightly upregulated the β-catenin activity. Transcription from the reporter plasmid containing the mutated Tcf/LEF-binding site was not affected by overexpression of β-catenin or Siah-1L protein. We also found that expressing Siah-1L in cells resulted in a dose-dependent reduction in the relative Tcf/LEF transcriptional activity induced by β-catenin (Figure 3b). In addition, a marked reduction in the levels of endogenous β-catenin protein was detectable in cells expressing Siah-1L compared to control or Siah-1ΔRING-expressing cells (Figure 3c). These findings indicate that Siah-1L regulates Tcf/LEF activity and β-catenin protein levels in cells.

Since a p53-activating stimulus was required for Siah-1L expression, we asked whether Siah-1L could reduce β-catenin activity in Hep3B cells that lack endogenous p53. As shown in Figure 3d, expression of β-catenin protein induced about a 20-fold in Tcf/LEF transcriptional activity. When an expression plasmid encoding Siah-1L was cotransfected, Tcf/LEF activity was reduced almost by half. Moreover, analysis of endogenous β-catenin levels demonstrated that exogenously expressed Siah-1L protein significantly reduced the amount of β-catenin (Figure 3e). Similar results were observed in H1299 cells, which lack p53 genes (data not shown). Thus, despite the deletion of the endogenous p53 genes, exogenous expression of Siah-1L resulted in the degradation of endogenous β-catenin protein, suggesting a role for Siah-1L as a negative regulator of β-catenin activity.

Mutant β-catenin found in some cancer cells is resistant to Siah-1L-induced protein degradation

Mutated β-catenin found in HepG2 cells is known to carry an activating mutation caused by the deletion of amino acids 25–140 (de La Coste et al., 1998). This mutant β-catenin is known to be resistant to GSK3β-mediated degradation, resulting in an aberrant accumulation of β-catenin (de La Coste et al., 1998). To determine whether Siah-1-family proteins can regulate the activity of mutated β-catenin, we examined the effects of Siah-1L expression on mutant β-catenin protein in HepG2 cells, which have wild-type p53 gene.

Figure 2 p53 specifically enhances the expression of Siah-1L and is involved in the regulation of β-catenin protein degradation via Siah-1L. MCF7 and Hep3B cells were transfected with pRC-CMV-p53 (wild type) (p53), pRC-CMV-p53 (Mut178) (Mut-p53), or empty vector (CTR). (a) Total RNA was prepared from MCF7 cells 24 h after transfection, and RT–PCR was performed using specific primers for Siah-1L (upper panel), Siah-1 (middle panel), and GAPDH (lower panel). (b) MCF7 cells were cotransfected with pPUR and expression plasmids encoding wild-type p53 (p53), p53 mutant (Mut-p53), or empty vector (CTR). After 24 h, puromycin (2.0 μg/ml) was added to the medium and the cells were cultured continuously for 72 h. Cell lysates (5 μg) were analysed by Western blots using anti-β-catenin (upper panel), anti-p53 (middle panel), or anti-α-actin (lower panel) antibodies. (c) The levels of Siah-1L (upper panel) and Siah-1 (middle panel) mRNAs in total RNA isolated from Hep3B cells transfected with plasmids encoding wild-type p53 or mutant p53 were determined by RT–PCR. (d) Expression plasmids encoding wild-type or mutant p53 and pPUR were cotransfected into Hep3B cells, and puromycin (2.0 μg/ml) was added to the medium 24 h after transfection. After 72 h, total protein was isolated and analysed by Western blots using anti-β-catenin (upper panel) or anti-p53 (middle panel) antibodies. (e) HEK293T cells were transfected with the expression plasmids of FLAG-Siah-1L or -Siah-1 with or without siRNA for Siah-1L (siSiah-1L). Cells were cultured for 36 h in the presence of MG 132. Cell lysates were analysed by Western blots using anti-FLAG and anti-α-actin antibodies. siCTR represents a control siRNA. (f) Total RNA was isolated from HEK293T cells transfected with p53 expression plasmids with or without siRNA for Siah-1L (siSiah-1L). Control siRNA-transfected cells (siCTR) were used as a negative control. RT–PCR was performed using specific primers for Siah-1L (upper panel), Siah-1 (middle panel), or GAPDH (lower panel). (g) The siRNA for Siah-1L (siSiah-1L) or control siRNA (siCTR) was transfected in HEK293T cells. After 24 h, cells were transfected with the expression plasmids of Myc-tagged β-catenin (AAAA) with or without p53 expression plasmid and cultured for 36 h. Total protein was isolated from these cells and Western blots were performed using anti-Myc, anti-p53, and anti-α-actin. (h) Total protein was isolated from HEK293T cells transfected with Myc-tagged β-catenin (AAAA) and p53 expression plasmids with or without FLAG-tagged Siah-1ΔRING expression plasmid. Cell lysates were analysed by Western blots with antibodies against Myc, p53, FLAG, and α-actin
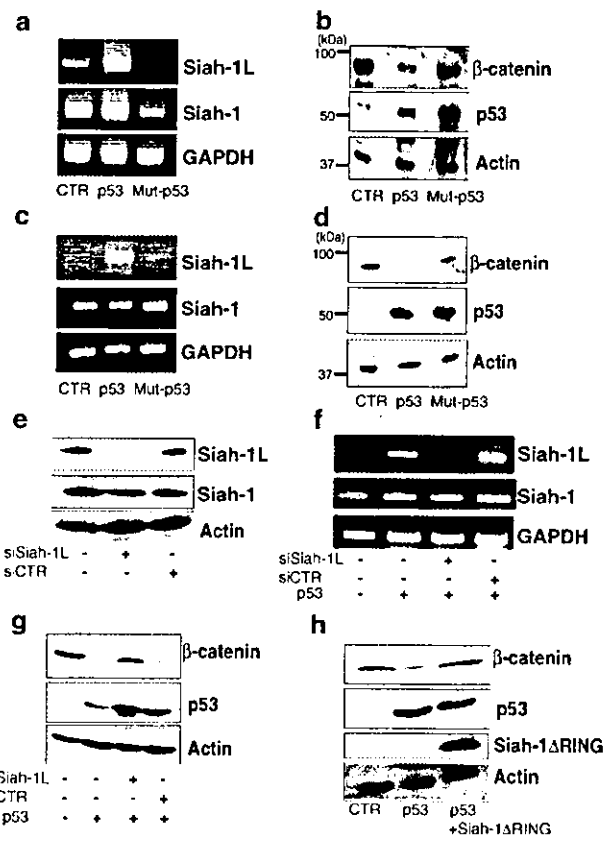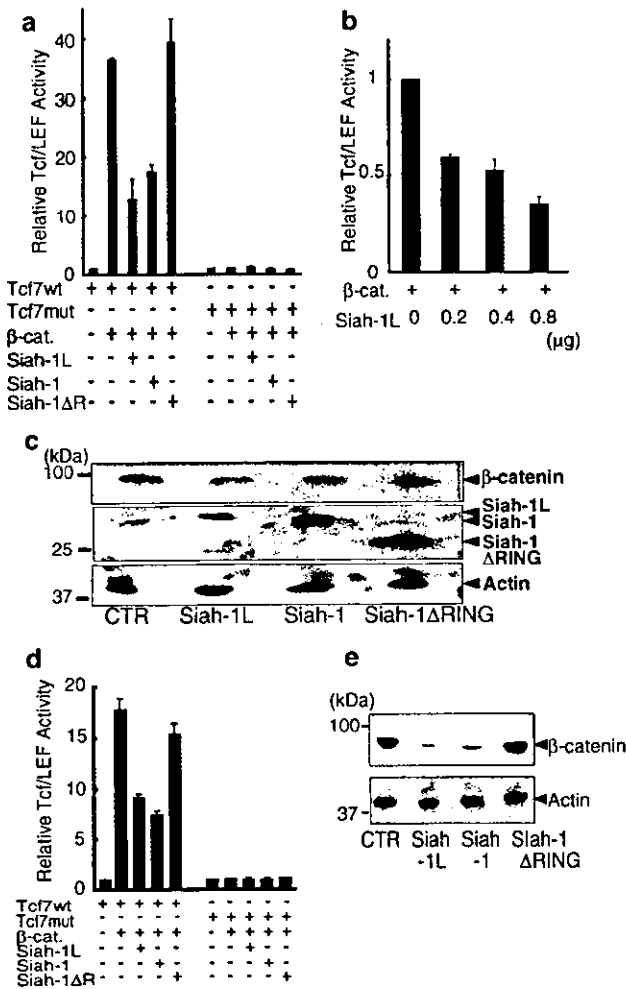
Figure 3 Effects of Siah-1L on Tcf/LEF reporter activity and β-catenin levels in cells with or without endogenous p53. (a) MCF7 cells were cotransfected with the pTcf7wt-Luc (Tcf7wt) reporter plasmid, together with plasmids encoding β-catenin (β-cat.) and Siah-1L (Siah-1L), Siah-1 (Siah-1), or Siah-1ΔRING (Siah-1ΔR). The pTcf7mut-Luc (Tcf7mut) reporter plasmid, which contains a mutated Tcf-binding motif, was used as a control. Reporter assays were performed as described in Materials and methods. (b) MCF7 cells were transfected with the pTcf7wt-Luc reporter plasmid, pcDNA3-Myc-β-catenin (β-cat.), and increasing amounts of plasmid encoding Siah-1L (Siah-1L) (0–0.8 μg), followed by reporter assays. (c) MCF7 cells were transfected with pPUR and empty vector (CTR), pcDNA3-FLAG-Siah-1L (Siah-1L), pcDNA3-FLAG-Siah-1 (Siah-1), or pcDNA3-FLAG-Siah-1ΔRING (Siah-1ΔRING) expression plasmids. Puromycin (3.0 μg/ml) was added 24 h later, and cell lysates were prepared after another 72 h of culture in the presence (probed with anti-FLAG) or absence (probed with anti-β-catenin or anti-α-actin) of MG132. Lysates were subjected to Western blot analyses using anti-β-catenin (upper panel), anti-FLAG (middle panel), or anti-α-actin (Actin) (lower panel) antibodies. (d) Hep3B cells were transfected with the pTcf7wt-Luc (Tcf7wt) reporter plasmid, pcDNA3-Myc-β-catenin (β-cat.), and plasmids encoding Siah-1L (Siah-1L), Siah-1 (Siah-1), or Siah-1ΔRING (Siah-1ΔR). Transcriptional activities were measured by reporter assays. (e) Hep3B cells were transfected with pPUR and empty vector (CTR) or expression plasmids encoding Siah-1L (Siah-1L), Siah-1 (Siah-1), or Siah-1ΔRING (Siah-1ΔRING). After 24 h, puromycin was added to the medium and culture was continued for 36 h. Cell lysates were prepared, normalized for total protein content (10 μg per lane), and analysed by Western blots using β-catenin antibody
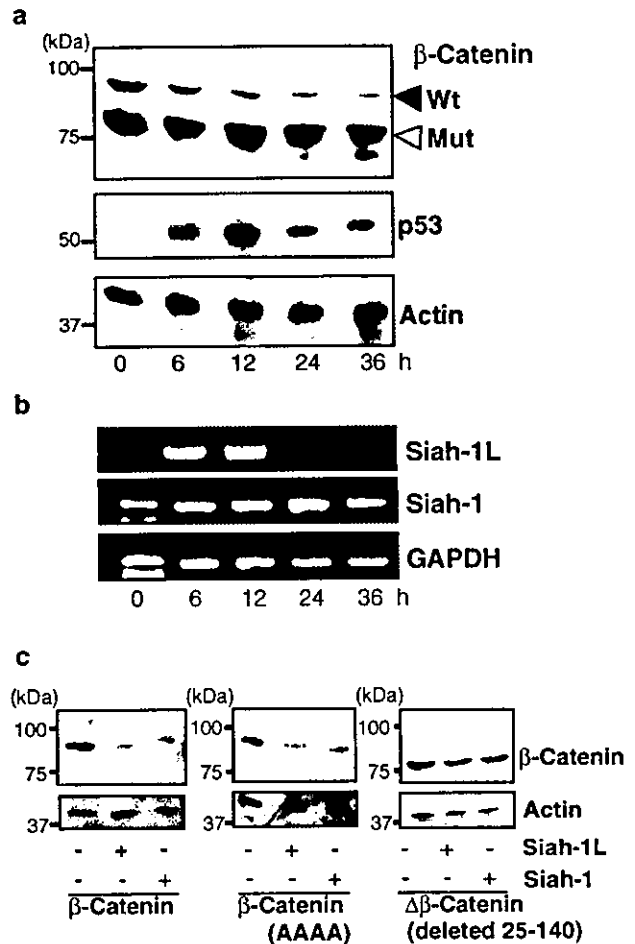
Figure 4 β-Catenin with a deletion mutation is resistant to Siah-1L-induced degradation. (a) Total protein was isolated from HepG2 cells immediately before (0 h) and 6, 12, 24, and 36 h after treatment with DOX (15 μg/ml). Western blot analyses using anti-β-catenin, anti-p53 (p53), or anti-α-actin (Actin) antibody were performed. The closed arrowhead shows wild-type β-catenin (Wt) and the open arrowhead shows the β-catenin deletion mutant (Mut). (b) Total RNA was prepared from HepG2 cells before (0 h) and 6, 12, 24, and 36 h after treatment with DOX (15 μg/ml). The levels of Siah-1L (upper panel), Siah-1 (middle panel), and GAPDH (lower panel) mRNAs were analysed by RT–PCR. (c) HEK293T cells were transfected with pcDNA3-Myc-β-catenin, pcDNA3-Myc-β-catenin (AAAA), or pcDNA3-Myc-Δβ-catenin (deleted 25–140) and empty vector (CTR) or plasmids encoding each Siah-family protein. A 10 μg portion of cellular lysates was resolved on SDS–PAGE and immunoblotted with antibodies against Myc or α-actin (Actin)

As shown in Figure 4a, the endogenous expression of both wild-type and mutant β-catenin proteins was observed in cells. The levels of endogenous p53 protein were markedly increased after DOX treatment (Figure 4a, middle panel). The amount of Siah-1L mRNA was strongly upregulated in response to DOX, whereas the level of Siah-1 transcript remained unchanged (Figure 4b). Interestingly, the degradation of wild-type β-catenin protein in HepG2 cells was observed after p53 activation induced by DOX. However, the expression of mutant β-catenin protein remained unchanged (Figure 4a, upper panel) and levels of Tcf/LEF

activity remained unchanged in cells overexpressing Siah-1L or Siah-1 (data not shown). We then investigated the ability of Siah-1L to induce degradation of transiently overexpressed Δβ-catenin (deleted 25–140) or mutant β-catenin (AAAA). As shown in Figure 4c, both Siah-1L and Siah-1 markedly reduced the levels of wild-type β-catenin and β-catenin (AAAA), while the levels of Δβ-catenin (deleted 25–140) remained unchanged. Taken together, these results indicate that β-catenin lacking amino acids 25–140 is resistant to Siah-1-dependent degradation pathways.

Siah-1L sensitizes cancer cells to apoptosis induced by anticancer drugs

To explore the functional significance of p53-inducible Siah-1L in tumor cell survival, we evaluated the ability of Siah-1L to promote apoptosis. MCF7 cells were transiently transfected with plasmids encoding Siah-1L, Siah-1, or Siah-1ΔRING, and cell death was measured 48 h after treatment with DOX. As shown in Figures 5a and b, Siah-1L and Siah-1 enhanced cell death by greater than 50% compared to the control and Siah-1ΔRING-expressing cells. Interestingly, apoptosis-sensitizing effects induced by Siah-1L protein were also observed in p53-null cells (Figures 5c and d). Moreover, similar results were obtained when cell death was induced by cisplatin or UV irradiation in MCF7 and Hep3B cells (data not shown). These data strongly suggest that Siah-1L accelerates cell death induced by anticancer drugs irrespective of the status of endogenous p53 protein.
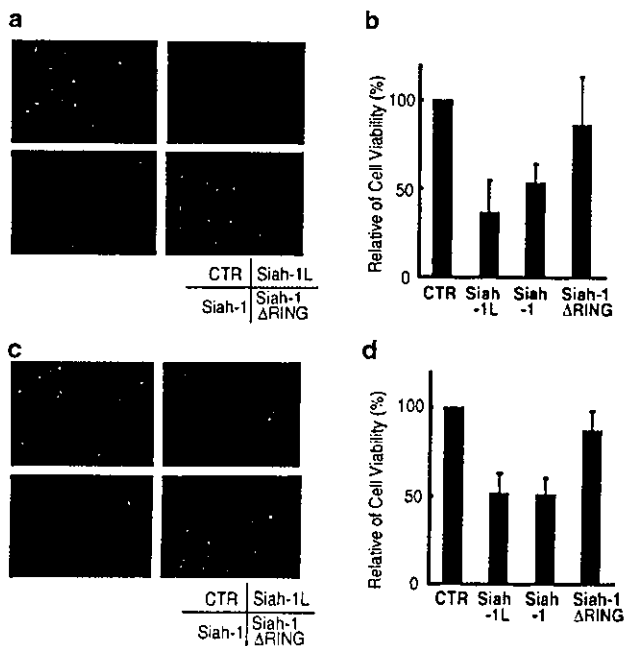

Figure 5 Siah-1L sensitizes cancer cells to apoptotic cell death. MCF7 (a, b) or Hep3B (c, d) cells were treated with DOX (1.0 μg/ml) 24 h after transfection of pEGFP-C1 together with empty vector (CTR), pcDNA3-FLAG-Siah-1L (Siah-1L), pcDNA3-FLAG-Siah-1 (Siah-1), or pcDNA3-FLAG-Siah-1ΔRING (Siah-1ΔRING). After 48 h, the GFP-positive viable cells were counted and the relative number of GFP-positive cells was presented

Discussion

It has been suggested that Siah-1 may act as a downstream effector of p53; however, the 5′-flanking region of the Siah-1 gene is known to lack typical TATA or CCAAT boxes and that reporter plasmids containing the promoter region of Siah-1 do not respond to p53 (Maeda et al., 2002). Recently, the p53-responsive element has been identified upstream of the alternative in-frame ATG start codon located in the intron 1 of the human Siah-1 gene (Matsuzawa et al., unpublished data). In this study, we demonstrated that a novel isoform belonging to the human Siah-1 family, Siah-1L, was identified as a p53-inducible protein.

· Dysfunction of the β-catenin degradation pathway results in aberrant accumulation of β-catenin; this is a frequent event in various human cancers, and the aberrant accumulation of β-catenin is reported to trigger oncogenesis and tumor progression (Chung, 2000; Lin et al., 2000; Park et al., 2001; Ueda M et al., 2001; Inagawa et al., 2002). However, it has also been shown that aberrant accumulation of β-catenin is not always accompanied by known dysfunction or mutation of the APC, Axin, or β-catenin genes. Recently, Cagatay and Ozturk (2002) demonstrated that aberrant accumulation of β-catenin in tumors is often associated with inactivation of the p53 gene. They also showed that worldwide p53 and β-catenin mutation rates are inversely correlated in HCC (Cagatay and Ozturk, 2002). These data suggest that inactivation of p53 may be an important cause of aberrant accumulation of β-catenin in cancer cells. However, the molecular mechanism by which p53 regulates β-catenin activity has been unclear. In this study, we have demonstrated that the expression level of Siah-1L is regulated in a p53-dependent manner in cells with wild-type p53. In contrast, in p53-null cells, no induction of Siah-1L was observed after p53-activating stimuli, resulting in the sustained accumulation of β-catenin protein. Moreover, using specific siRNA for Siah-1L, p53-induced degradation of β-catenin was almost rescued. These results suggest that lack of Siah-1L, but not Siah-1, expression in response to p53 may contribute to the aberrant accumulation of β-catenin in cells harboring p53 mutations. It is important to note that overexpression of Siah-1L in p53-null cells led to the degradation of the accumulated endogenous β-catenin protein, indicating that aberrant accumulation of β-catenin can be reversed by exogenously expressed Siah-1-family proteins in cancer cells regardless of p53 status.

β-Catenin with mutations in the GSK3β phosphorylation sites has been observed in various human cancers. For example, mis-sense mutations at codons 32, 34, 37, or 41, which affect the GSK3β phosphorylation sites of β-catenin, were also common in HCC (Wong et al., 2001; Cagatay and Ozturk, 2002). Siah-family proteins trigger the degradation of β-catenin protein regardless of the GSK3β-mediated phosphorylation of β-catenin. Thus, our data indicate that activation of Siah-1L-dependent β-catenin degradation, including the overexpression of exogenous Siah-1L proteins, may

represent a powerful approach to the treatment of cancers with aberrant accumulation of β-catenin and dysregulated Wnt/β-catenin signalling. On the other hand, constitutive activation of β-catenin caused by deletions in exons 3 and 4 was found in some human cancers (de La Coste et al., 1998). Therefore, we must draw attention to the finding that overexpression of Siah-1-family protein had little effect on the degradation of this mutant β-catenin found in HepG2 cells. Further analysis of the Siah-1/SIP/Ebi pathway for β-catenin degradation is necessary to find a strategy to counteract the various types of mutant β-catenin protein.

We have concluded that p53-dependent expression of Siah-1L but not Siah-1 plays an important role in the regulation of β-catenin activity in human tumor cells. These results suggest new strategies for restoring tumor suppressive pathways caused by p53 inactivation.

Materials and methods

Plasmids

The cDNA encoding human Siah-1L was generated by RT-PCR from the mRNA of MCF7 cells treated with DOX using SuperScript II (Invitrogen, San Diego, CA, USA), followed by PCR amplification using the KOD-Plus-DNA polymerase system (TOYOBO, Osaka, Japan) and the following oligonucleotide primers: 5'-GACGAATTCATGGTTATAATTAT TTTTCT-3' (sense) and 5'-GACCTCGAGTCAACACATGG AAATAGTTAC-3' (antisense). The resulting PCR fragments were inserted into the EcoRI–XhoI sites of pcDNA3-FLAG (Matsuzawa and Reed, 2001). pcDNA3-FLAG-Siah-1 and pcDNA3-FLAG-Siah-1ΔRING plasmids were constructed by inserting the EcoRI–XhoI fragments from the pcDNA3-Myc-Siah-1 and pcDNA3-Myc-Siah-1ΔRING plasmids into the pcDNA3-FLAG vector (Matsuzawa and Reed, 2001). pRC-CMV-p53 (wild type) and pRC-CMV-p53 (179Mut) were described previously (Unger et al., 1992). The expression plasmid encoding β-catenin, pcDNA3-Myc-β-catenin, was described previously (Ueda Y et al., 2001). The cDNAs encoding various β-catenin mutants were generated by two-step PCR amplification. Briefly, to construct β-catenin (AAAA), which has alanine substitutions at the putative GSK3β phosphorylation sites (serine or threonine amino-acid residues at positions 33, 37, 41, and 45), a DNA fragment encoding amino acids 1–37, a fragment encoding amino acids 33–50, and a fragment encoding amino acids 44–781 were separately PCR amplified with the following primer sets: BCAT-fullS, 5'-GGATCCGTATGGCTACTCAAGCTGAT TT-3', BCAT-37AS, 5'-AGCATGGATTCCAGCGTCCAGG TAAGAC-3'; BCAT-33S, 5'-GCTGGAATCCATGCTGGT GCCACTGCCACTGCCACAGCT-3', BCAT-50AS, 5'-GCC TTTACCACTCAGAGCAGGAGCTGTGGCAGTGGC-3'; BCAT-44S, 5'-CCTGCTCTGAGTGGTAAAGGC-3', BCAT-fullAS, 5'-TCTAGATTACAGGTCAGTATCAAACC-3'. The resulting PCR fragments were mixed and subjected to a second PCR reaction to obtain full-length β-catenin (AAAA) containing BamHI and XbaI sites. To construct $\Delta\beta$-catenin (deleted 25–140), which lacks amino acids 25–140, DNA fragments encoding the amino- and carboxyl-terminal regions were separately PCR amplified with primer sets BCAT-fullS and BCAT-25AS (5'-GTGACTAACAGCCGCTTTTC-3') and BCAT-120S (5'-GTGTTGTTTTATGCCATTAC-3') and BCAT-fullAS, respectively. The two PCR products were

mixed and subjected to a second PCR reaction to obtain full-length $\Delta\beta$-catenin (deleted 25–140) containing BamHI and XbaI sites. These products were subcloned into the BamHI and XbaI sites of the pcDNA3-Myc plasmid (Matsuzawa and Reed, 2001). The reporter plasmids pTcf7wt-Luc and pTcf7mut-Luc have been described previously (Ueda Y et al., 2001). All constructs were confirmed by DNA sequencing.

Cell culture and transfection

Human breast cancer MCF7 cells, hepatoma Hep3B cells, hepatoblastoma HepG2 cells, and human embryonic kidney HEK293T cells were maintained in Dulbecco's modified Eagle's medium (Nissui, Tokyo, Japan) supplemented with 10% FBS, and L-glutamine at 37°C in an atmosphere containing 5% CO_2. In some cases, cells were exposed to DOX, $10 J/m^2$ UV irradiation, or $5 \mu M$ MG132 (Peptide Institute, Osaka, Japan). For transfection of plasmids into the cells, we used the FuGENE6 transfection reagent (Roche, Indianapolis, IN, USA) according to the manufacturer's protocol. The amount of plasmid DNA in each transfection was kept constant by the addition of an appropriate amount of empty expression vector.

siRNA transfections

We designed the following siRNA duplexes within the open reading frame of Siah-1L to knock down Siah-1L. The siRNA duplexes were synthesized and purified by Qiagen Inc. (Cambridge, MA, USA). Siah-1L target sequence was as follows: siSiah-1L, 5'-AACTCCTGCCTCCTTATGTATTT-3'. The nonsilencing siRNA (control siRNA) was as follows: siCTR, 5'-AAGAGCCGTCAGACTGCTACA-3'. For transient transfections, cells were seeded at a density of 40–50% in 60 mm diameter plates. The following day, transfections of siRNAs were performed by using Lipofectamine 2000 reagent (Invitrogen), according to the manufacturer's recommended protocol.

Preparation of RNA and RT–PCR

Total RNA was extracted using Sepasol-RNA I Super (Nacalai Tesque, Kyoto, Japan) according to the manufacturer's protocol. RT–PCR was performed using the One Step RNA PCR Kit (Takara, Tokyo, Japan) according to the manufacturer's protocol. The PCR primers for amplification of Siah-1L, Siah-1, and GAPDH were as follows: Siah-1L-3S, 5'-GGTTATAATTATTTTTCTCCTGCCTCC-3' and Siah-1&1L-512AS, 5'-AGTCAACAGCACCAGGAAGA-3'; Siah-1-minus18S, 5'-CGCTCTCCGCCCACAGAAAT-3' and Siah-1&1L-512AS; GAPDH-1S, 5'-ATGGGGAAGGTGAAGGT CGG-3' and GAPDH-837AS, 5'-TGGAGGGATCTCGCTC CTGG-3'.

Western blot analyses

Protein samples were diluted in 2 × sodium dodecyl sulfate (SDS) sample buffer (62.5 mM Tris-HCl, pH 6.8, 2% SDS, 5% β-mercaptoethanol, 10% glycerol, and 0.002% bromophenol blue). Samples were separated by 10% SDS–polyacrylamide gel electrophoresis (PAGE). After electrotransfer, polyvinylidene difluoride membranes were probed with primary antibodies and secondary antibodies conjugated to HRP. The antibodies used in these experiments were anti-β-catenin (Transduction Laboratories, Lexington, KY, USA), anti-p53 (Ab-6) (Calbiochem), anti-c-Myc (9E10) (Santa Cruz Biotechnology Inc., Santa Cruz, CA, USA), anti-FLAG M2 (Sigma, St Louis, MO, USA), anti-α-actin (Sigma), and goat

polyclonal anti-Siah-1 (Abcam, Cambridge, UK). Immuno-complexes were detected by the enhanced chemiluminescence assay (NEN Life Science, Boston, MA, USA).

Reporter assays

To determine Tcf/LEF activity, subconfluent cells were transfected with a reporter construct (pTCF7wt-Luc or pTCF7mut-Luc) and various expression plasmids. A thymidine kinase (TK)-expressing vector (pRL-TK; Promega, Madison, WI, USA) was included as an internal control for transfection efficiency. After 30 h, the cells were lysed and both the luciferase and TK activities were determined using a luciferase assay kit (Promega). Tcf/LEF reporter activities were normalized relative to TK activities and were presented as mean±s.d. from at least three independent experiments.

Evaluation of cell death

MCF7 and Hep3B cells were grown on plastic dishes as monolayers. Cells were transfected with pEGFP-Cl (BD Biosciences Clontech) and various expression plasmids encoding Siah-1L, Siah-1, or Siah-1ΔRING or empty vector (CTR) for 12 h, followed by treatment with DOX. After 48 h, the GFP-positive cells were counted using a Zeiss AxioVert200 (Zeiss, Hallbergmoos, Germany). The histogram is presented as the average±s.d. of three independent experiments,

and the relative survival rate was determined by normalizing to the number of GFP-positive cells transfected with empty vector.

Abbreviations

APC, adenomatous polyposis coli; GSK3β, glycogen synthase kinase 3β; SIP, Siah interacting protein; HCC, hepatocellular carcinoma; RT-PCR, reverse-transcriptase polymerase chain reaction; DOX, doxorubicin; siRNA, short interfering RNA; Tcf, T-cell factors; LEF, lymphocyte enhancer-binding factor; SDS-PAGE, sodium dodecyl sulfate-polyacrylamide gel electrophoresis; TK, thymidine kinase.

Acknowledgements

References

Cagatay T and Ozturk M. (2002). Oncogene, 21, 7971–7980.

Chung DC. (2000). Gastroenterology, 119, 854–865.

de La Coste A, Romagnolo B, Billuart P, Renard CA, Buendia MA, Soubrane O, Fabre M, Chelly J, Beldjord C, Kahn A and Perret C. (1998). Proc. Natl. Acad. Sci. USA, 95, 8847–8851.

Della NG, Senior PV and Bowtell DD. (1993). Development, 117, 1333–1343.

Devereux TR, Stern MC, Flake GP, Yu MC, Zhang ZQ, London SJ and Taylor JA. (2001). Mol. Carcinogen., 31, 68–73.

Fiucci G, Beaucourt S, Duflaut D, Lespagnol A, Stumptner-Cuvelette P, Geant A, Buchwalter G, Tuynder M, Susini L, Lassalle JM, Wasylyk C, Wasylyk B, Oren M, Amson R and Telerman A. (2004). Proc. Natl. Acad. Sci. USA, 101, 3510–3515.

Hart MJ, de los Santos R, Albert IN, Rubinfeld B and Polakis P. (1998). Curr. Biol., 8, 573–581.

Hu G, Chung YL, Glover T, Valentine V, Look AT and Fearon ER. (1997a). Genomics, 46, 103–111.

Hu G, Zhang S, Vidal M, Baer JL, Xu T and Fearon ER. (1997b). Genes Dev., 11, 2701–2714.

Inagawa S, Itabashi M, Adachi S, Kawamoto T, Hori M, Shimazaki J, Yoshimi F and Fukao K. (2002). Clin. Cancer Res., 8, 450–456.

Lee TK, Lau TC and Ng IO. (2002). Cancer Chemother. Pharmacol., 49, 78–86.

Lin SY, Xia W, Wang JC, Kwong KY, Spohn B, Wen Y, Pestell RG and Hung MC. (2000). Proc. Natl. Acad. Sci. USA, 97, 4262–4266.

Liu J, Stevens J, Rote CA, Yost HJ, Hu Y, Neufeld KL, White RL and Matsunami N. (2001). Mol. Cell, 7, 927–936.

Maeda A, Yoshida T, Kusuzaki K and Sakai T. (2002). FEBS Lett., 512, 223–226.

Matsuzawa S and Reed JC. (2001). Mol. Cell, 7, 915–926.

Matsuzawa S, Takayama S, Froesch BA, Zapata JM and Reed JC. (1998). EMBO J., 17, 2736–2747.

Omer CA, Miller PJ, Diehl RE and Kral AM. (1999). Biochem. Biophys. Res. Commun., 256, 584–590.

Park WS, Oh RR, Park JY, Kim PJ, Shin MS, Lee JH, Kim HS, Lee SH, Kim SY, Park YG, An WG, Jang JJ, Yoo NJ and Lee JY. (2001). J. Pathol., 193, 483–490.

Peifer M and Polakis P. (2000). Science, 287, 1606–1609.

Provost E and Rimm DL. (1999). Curr. Opin. Cell Biol., 11, 567–572.

Relaix F, Wei X-J, Li W, Pan J, Lin Y, Bowtell DD, Sassoon DA and Wu X. (2000). Proc. Natl. Acad. Sci. USA, 97, 2105–2110.

Roperch JP, Lethrone F, Prieur S, Piouffre L, Israeli D, Tuynder M, Nemani M, Pasturaud P, Gendron MC, Dausset J, Oren M, Amson RB and Telerman A. (1999). Proc. Natl. Acad. Sci. USA, 96, 8070–8073.

Satoh S, Daigo Y, Furukawa Y, Kato T, Miwa N, Nishiwaki T, Kawasoe T, Ishiguro H, Fujita M, Tokino T, Sasaki Y, Imaoka S, Murata M, Shimano T, Yamaoka Y and Nakamura Y. (2000). Nat. Genet., 24, 245–250.

Ueda M, Gemmill RM, West J, Winn R, Sugita M, Tanaka N, Ueki M and Drabkin HA. (2001). Br. J. Cancer, 85, 64–68.

Ueda Y, Hijikata M, Takagi S, Takada R, Takada S, Chiba T and Shimotohno K. (2001). Biochem. Biophys. Res. Commun., 283, 327–333.

Unger T, Nau MM, Segal S and Minna JD. (1992). EMBO J., 11, 1383–1390.

Wong CM, Fan ST and Ng IO. (2001). Cancer, 92, 136–145.

Yost C, Torres M, Miller JR, Huang E, Kimelman D and Moon RT. (1996). Genes Dev., 10, 1443–1454.

The Role of Notch Signaling in the Development of Intrahepatic Bile Ducts

YUZO KODAMA,*,† MAKOTO HIJIKATA,† RYOICHIRO KAGEYAMA,§ KUNITADA SHIMOTOHNO,† and TSUTOMU CHIBA*

*Department of Gastroenterology and Hepatology, School of Medicine; †Laboratory of Human Tumor Viruses, Department of Viral Oncology; and §Laboratory of Growth Regulation, Department of Cell Biology, Institute for Virus Research, Kyoto University, Kyoto, Japan

Background & Aims: Mutations in *Jagged1*, a Notch ligand, cause Alagille syndrome (AGS), a disorder characterized by a paucity of intrahepatic bile ducts (IHBD). The mechanism underlying the contribution of the Notch signaling pathway to IHBD formation, however, remains unknown. Here we investigated the role of Notch signaling in IHBD development. *Methods:* The expression patterns of Jagged1, Notch2, and Hes1 during mouse liver development were analyzed by semiquantitative reverse-transcription polymerase chain reaction (RT-PCR), immunoblot, and immunohistochemistry. The hepatocyte maturation level and IHBD development were studied in *Hes1* null mice in comparison with wild-type mice. The effect of Jagged1 on biliary differentiation was assessed by using an in vitro 2-cell coculture system with WB-F344 cells, a cell line derived from normal adult rat liver. *Results:* Jagged1 was expressed in the portal mesenchyme during the neonatal period. During the same period, Notch2 and Hes1 expression was observed in the biliary epithelial cells adjacent to the Jagged1-positive cells. During ductal plate remodeling, Notch2 and Hes1 were up-regulated exclusively in the biliary epithelial cells that form tubular structures. In contrast, the tubular formation of IHBD was completely absent in *Hes1* null mice. Coculture with Balb3T3 cells stably overexpressing Jagged1 induced transactivation of the *Hes1* promoter and increased expression of biliary lineage markers, such as cytokeratin-19 and γ-glutamyl transpeptidase, in WB-F344 cells. *Conclusions:* Our results suggest that Notch signaling has an important role in the differentiation of biliary epithelial cells and is essential for their tubular formation during IHBD development.

Notch signaling is an evolutionarily conserved mechanism that regulates the determination of cell fate during the development of various tissues and organs.[1] The Notch family gene encodes large type I transmembrane receptors. To date, 4 Notch receptors have been identified in mammals, Notch1, 2, 3, and 4. Notch ligands are also type I transmembrane proteins. Currently, at least 5 ligands have been identified, including Jagged1, Jagged2, Delta-like1, Delta-like3, and Delta-like4. Activation of Notch receptors, by binding with ligands expressed on adjacent cells, leads to proteolytic release and nuclear translocation of the intracellular domain of Notch. The intracellular domain of Notch acts as a transcriptional activator in cooperation with the classic DNA binding protein RBP-Jκ, and activates target genes such as *Hes1* and *Hes5*, which have a critical role in regulating differentiation.

Recently, it was shown that several human diseases are caused by mutations in components of the Notch signaling pathway. Mutations in the *Jagged1* gene are responsible for Alagille syndrome (AGS) (Online Mendelian Inheritance in Man 11850),[2,3] an autosomal-dominant disorder characterized by neonatal jaundice and a paucity of intrahepatic bile ducts (IHBD).[2–6] *Jagged1* mutations are detected in 60%–70% of patients with clinically confirmed AGS,[7–10] and a paucity of IHBD has been identified in 80%–85% of AGS patients.[6,11] Because several studies showed that the paucity is progressive with increasing age, impaired postnatal development of the bile duct is proposed as a mechanism of diminishing IHBD in AGS.[6,12] These genotypic and phenotypic findings in AGS suggest that Notch signaling has a crucial role in the human postnatal development of IHBD. On the other hand, although mice heterozygous for the *Jagged1* null mutation did not exhibit any IHBD-deficient phenotypes in the liver,[13] it was reported recently that mice doubly heterozygous for the *Jagged1* null allele and a *Notch2* hypomorphic allele exhibited abnormalities similar to those of AGS,[14] suggesting that the interaction between Jagged1 and Notch2 also is important in mouse IHBD development.

During mammalian liver development, IHBD arise from the hepatoblasts, which are precursor cells with the potential to differentiate into either hepatocytes or biliary epithelial cells.[15,16] First, hepatoblasts in contact with the portal mesenchyme differentiate into biliary epithelial cells. These cells then form a single cell layer, called the ductal plate, around the portal vein, and then progressive remodeling of the ductal plate occurs. Short segments of the ductal plate dilate to form tubular structures, which subsequently are incorporated into the portal mesenchyme, whereas the nontubular parts of the ductal plate gradually disappear. Finally, the tubular structures develop into mature bile ducts in the portal mesenchyme. Although it has been suggested that epithelial-mesenchymal interactions between biliary epithelial cells and portal mesenchyme are crucial to IHBD development, their molecular mechanisms are mostly unknown.[15,17]

In the present study, we analyzed the expression patterns of Notch signaling components, especially Jagged1, Notch2, and their main downstream molecule, Hes1, during mouse liver development to elucidate the role of Notch signaling in IHBD development. Also, by analyzing the phenotype of *Hes1* null mice, we investigated the involvement of Notch signaling in IHBD development. Furthermore, we studied the effect of Notch signaling on biliary differentiation of liver precursor cells in vitro.

Materials and Methods

Animals and Tissue Preparation

The liver tissues were prepared from fetal (embryonal day [ED] 11.5, ED13.5, ED15.5, and ED18.5; day of the discovery of the vaginal plug was defined as ED 0), postnatal, and adult (postnatal day [P] 1, P4, P7, P10, P14, P28, and P56; day of birth was defined as P0) ICR (an outbred Institute for Cancer Research strain) mice that were purchased from Japan SLC (Shizuoka, Japan). *Hes1* mutant mice were obtained and genotyped as previously reported.[18]

Cell Culture

WB-F344 cells were kindly provided by Dr. J. W. Grisham (University of North Carolina, Chapel Hill, NC). Cells were cultured in Ham's F12 medium (Invitrogen Corporation, Carlsbad, CA) supplemented with 5% fetal bovine serum. Jagged1-expressing Balb3T3 cells were kindly provided by Dr. S. Sakano (Asahi Kasei Corporation, Shizuoka, Japan). Briefly, Balb3T3 cells were stably transfected with a full-length human Jagged1 complementary DNA that is cloned into pMKITneo expression vectors.[19] After G418 selection (200 μg/mL), a clone was selected for further studies and named Balb3T3-Jagged1. Control cells were Balb3T3 cells that were transfected with empty vectors, selected as described earlier, and named Balb3T3-control. These cells were cultured in Dulbecco's modified Eagle medium (Nissui, Tokyo, Japan) supplemented with 10% fetal bovine serum, L-glutamine (584 μg/mL), and G418 (200 μg/mL).

RNA Extraction and Semiquantitative Reverse-Transcription Polymerase Chain Reaction

Total RNA was extracted from whole liver tissues of mice or from culture cells by using the acid guanidinium-phenol-chloroform method (Sepasol-RNA1; Nacalai Tesque, Kyoto, Japan). A 1-step reverse-transcription polymerase chain reaction (RT-PCR) method was performed by using a One-Step RNA PCR Kit (AMV; TaKaRa Biomedicals, Shiga, Japan) according to the manufacturer's directions. The number of cycles required to reach the midlogarithmic phase of amplification was determined for each amplicon. Primer sequences were 5'-ATCTGTCCACCTGGCTATGCAG-3' and 5'-ATCACTTCGCAGGTGGTGGTAC-3' (mouse *Jagged1*), 5'-TGACTCTATCCCCCGTCGATTC-3' and 5'-ACTGGA-TGTAACCTGCCCAAGC-3' (mouse *Notch2*), 5'-CCAAGC-TAGAGAAGGCAGACATTC-3' and 5'-TATTTCCCCAAC-ACGCTCG-3' (mouse *Hes1*), 5'-GAGAAAAACCGACTGC-GGAAG-3' and 5'-TGTAGTCCTGGTGCAGGCTCTT-3' (mouse *Hes5*), 5'-ACTCACCCCAACCTTCCTGTC-3' and 5'-CAGCAGTGGCTGATACCAGAG-3' (mouse α-fetoprotein), 5'-CATGACACCATGCCTGCTGAT-3' and 5'-CTCTGAT-CTTCAGGAAGTGTAC-3' (mouse albumin), 5'-TCGATC-CTAAGCACACTGAGG-3' and 5'-CGGCTTGTAAGACT-GTAGC-3' (mouse α1-antitrypsin), 5'-GCAGATGCTTCCT-TCAGACTG-3' and 5'CCACCAGGGCTTTGGAGATC-3' (mouse dipeptidylpeptidase IV), 5'-TGTGTTCAGTAAGCG-GCACCT-3' and 5'-CCCGAATCTCATTGCCAAAA-3' (mouse tyrosine aminotransferase), 5'-AACCCATTGTGAGGCCAG-AGG-3' and 5'-TACTCATTACACTAGTTGGTC-3' (mouse glucose-6-phosphatase), 5'-CGTGGGCCGCCCTAGGCA-CCA-3' and 5'-TTGGCCTTAGGGTTCAGGGCGG-3' (mouse β-actin).

Real-Time Quantitative RT-PCR

Real-time RT-PCR amplification and data analysis were performed using an ABI Prism 7700 Sequence Detector System (PE Applied Biosystems, Foster City, CA) as described previously.[20] PCR primers and probes for rat albumin (forward, 5'-AGTGTTTCCTGCAGCACAAGG-3'; reverse, 5'-GCCTCCGGCCTCTGGA-3'; fluorogenic probe, 5'-TGA-CAACCCCAACCTGCCACCC-3'), rat cytokeratin-19 (forward, 5'-CAGATCGACAATGCCCGC-3'; reverse, 5'-AG-GCCCTGTTCTGTCTCAAACT-3'; fluorogenic probe, 5'-AGAGCTGTGGAGGAGCCCCGTCTT-3'), rat γ-glutamyl transpeptidase (forward, 5'-TGTGGTTCGGGTATGAT-GTGA-3'; reverse, 5'-ATTGGGCAAAAGCTGGTTGT-3'; fluorogenic probe, 5'-TGGCTGCAGATGACTTGCGGACC-3') and rat 18S ribosomal RNA (forward, 5'-TAGAGTGT-TCAAAGCAGGCCC-3'; reverse, 5'-CCAACAAAATAGA-ACCGCGGT-3', fluorogenic probe, 5'-CGCCTAGATACCG-

CAGCTAGGAATAATG-3') were designed using the Primer Express program (PE Applied Biosystems).

Immunoblot Analysis

Immunoblot analysis was performed as described previously.[21] The primary antibodies used in these experiments were rabbit polyclonal antibody against mouse Hes1 (kindly supplied by Dr. T. Sudo, Toray Industries, Tokyo, Japan; final dilution, 1:1000)[22] and mouse monoclonal antibody against α-tubulin (Oncogene Research Products, San Diego, CA; final dilution, 1:3000).

Immunohistochemistry of Liver Tissues

The liver tissues from ICR mice and *Hes1*-deficient mice were fixed with phosphate-buffered 4% paraformaldehyde, embedded in paraffin, and cut at a thickness of 4 μm. The sections were dewaxed in xylene and rehydrated through a graded series of ethanol washes. For detection of Jagged1 protein, the sections were treated with proteinase K (Dako, Glostrup, Denmark) for antigen retrieval, then treated with 0.3% H_2O_2 in methanol to quench endogenous peroxidase activity. Slides were washed and incubated with a goat polyclonal antibody against Jagged1 (R&D Systems, Minneapolis, MN) at a final concentration of 1 μg/mL. After washing, they were incubated with biotinylated anti-goat immunoglobulin G (IgG; Jackson ImmunoResearch, West Grove, PA), followed by incubation with peroxidase-conjugated streptavidin (Dako). Staining was visualized using 3,3'-diaminobenzidine tetrahydrochloride color substrate (Dako) and counterstained with Mayer's hematoxylin. For detection of Notch2 and keratin proteins, rabbit polyclonal antibody against Notch2 (Santa Cruz Biotechnology, Santa Cruz, CA; final dilution, 1:100) and rabbit polyclonal antibody against bovine keratins (Dako; final dilution 1:3000) were used, respectively. Antigen retrieval and endogenous peroxidase blocking were performed as described earlier. The sections were immunostained using an EnVision+ kit (Dako) according to the manufacturer's instructions. For detection of Hes1 protein, rabbit polyclonal antibody against mouse Hes1 (final dilution, 1:1000) was used. To release the antigen, the slides were autoclaved at 121°C for 10 minutes. The sections then were immunostained by using an EnVision+ kit as described earlier.

Dual Immunofluorescence of Liver Tissues

Double immunostaining for Jagged1 and keratin was performed. The liver sections were prepared as described earlier. The primary antibody combination consisting of the goat anti-Jagged1 (final concentration, 1 μg/mL) and the rabbit polyclonal antibody against bovine keratins (final dilution, 1:3000) was used. Then primary antibodies were visualized by using the Alexa Fluor 568 donkey anti-goat IgG conjugate (red fluorescence; Molecular Probes, Eugene, OR) and fluorescein isothiocyanate–conjugated donkey anti-rabbit IgG (Jackson ImmunoResearch) on an Axiovert fluorescence microscope (Carl Zeiss, Jena, Germany).

Periodic Acid Schiff Staining and Lectin Histochemistry

The liver sections were prepared as described earlier. Intracellular glycogen was stained with the periodic acid Schiff (PAS) staining solution (Muto Pure Chemicals, Tokyo, Japan) according to the standard protocol.[23] For lectin binding, biotinylated *Dolichos biflorus* agglutinin (Vector Laboratories, Burlingame, CA) was used at a final concentration of 20 μg/mL. For detection of lectin binding, peroxidase-conjugated streptavidin (Dako) was used.

Immunofluorescence of Culture Cells

Membrane localization of Jagged1 was assessed by indirect immunofluorescence without permeabilization. Balb3T3 Jagged1 or Balb3T3 control cells were fixed with 4% paraformaldehyde. Cells were washed and incubated with the goat anti-Jagged1 antibody (final concentration, 1 μg/mL). After washing, they were incubated with the Alexa Fluor 568 donkey anti-goat IgG conjugate (red fluorescence, Molecular Probes) and 4',6-diamidino-2-phenylindole dihydrochloride. After washing, slides were mounted and viewed with an Axiovert fluorescence microscope (Carl Zeiss).

Transfection and Reporter Assays

Reporter plasmids under the control of the *Hes1* promoter (Hes1-luc),[24] were kindly provided by Dr. T. Honjo (Kyoto University, Kyoto, Japan). WB-F344 cells (1.0 × 10⁵) were transfected with *Hes1* promoter cells by using the FuGENE6 transfection reagent (Roche, Indianapolis, IN) according to the manufacturer's protocol. After 12 hours, no cells, 1.0 × 10⁵ Balb3T3 control cells, or 1.0 × 10⁵ Balb3T3 Jagged1 cells were added and cocultured in WB-F344 medium. To evaluate the possibility of the presence of a soluble factor as a mediator of *Hes1* promoter activation, 2 cells were cocultured with or without separation using a transwell membrane (Cell Culture Insert; Becton Dickinson, Franklin Lakes, NJ). After 24 hours of cocultivation, the reporter assay was performed as described previously.[25]

Differentiation Assay

WB-F344 cells (3.0 × 10⁵) were plated on a 10-cm diameter plate. After 12 hours, 3.0 × 10⁵ Balb3T3 control cells or 3.0 × 10⁵ Balb3T3 Jagged1 cells were added and cocultured in WB-F344 medium. After 3 days of cocultivation, total messenger RNA (mRNA) was extracted and analyzed for the expression of albumin, cytokeratin-19, or γ-glutamyl transpeptidase by real-time quantitative RT-PCR.

Results

Jagged1 Expression in the Portal Mesenchyme in the Neonatal Period

First, we analyzed the mRNA expression of α-fetoprotein, albumin, α1-antitrypsin, and *Jagged1* in total RNA extracted from fetal, neonatal, and adult

mouse liver by semiquantitative RT-PCR. α-fetoprotein (a marker of immature hepatocytes), albumin (a marker for immature to mature hepatocytes), and α1-antitrypsin (a marker of mature hepatocytes) mRNAs were detected in the expected patterns, suggesting that these serial RNA samples reflected period-specific characteristics (Figure 1A). Under these conditions,

although Jagged1 mRNA was detected throughout the entire period from fetus to adult, its concentration was highest in the neonatal period (P1, P7; Figure 1A). The localization of Jagged1 protein in this period (P7) was analyzed by immunohistochemistry. Jagged1 protein was detected in the portal veins, hepatic arteries, and periportal connective tissue, but not in the central veins, hepatocytes, or bile ducts (Figure 1B). Similar to Jagged1 mRNA expression, Jagged1 protein expression increased during the late fetal (ED18.5) to neonatal (P7) period (Figure 1C). Further, dual immunofluorescence staining for Jagged1 and keratin in this period revealed prominent Jagged1-expressing cells adjacent to the biliary epithelial cells, which were developing into IHBD (Figure 1D). Thus, Jagged1 was expressed predominantly in the portal mesenchyme of the neonatal liver such as portal veins, hepatic arteries, and periportal connective tissue, adjacent to the developing IHBD.
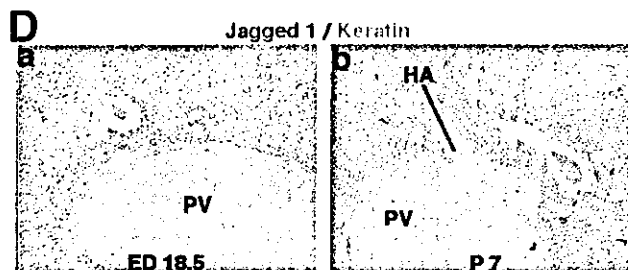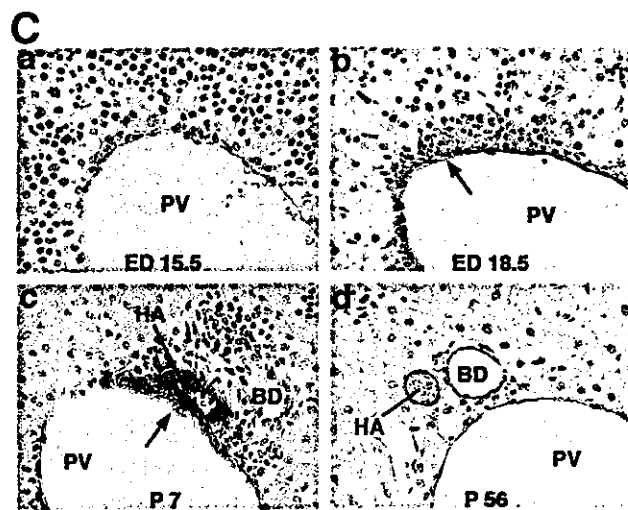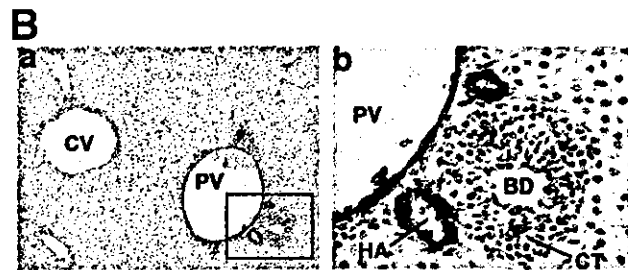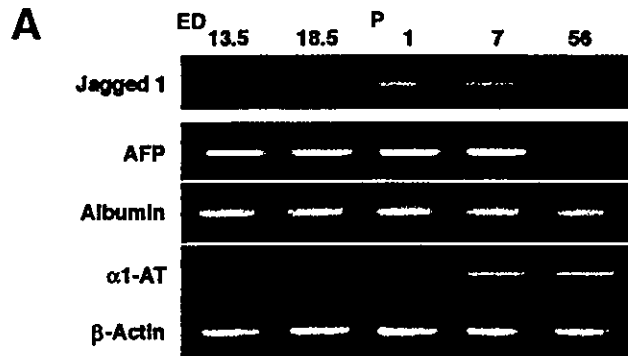
Notch2 Expression in the Biliary Epithelial Cells That Form Tubular Structures

Notch2 expression then was analyzed by semiquantitative RT-PCR and immunohistochemistry. Although Notch2 mRNA was detected during the entire period from fetus to adult, its expression was highest in the neonatal period, similar to Jagged1 (Figure 2A). In the immunohistochemical analysis, similar to Notch2 mRNA expression, Notch2 protein was not observed in fetal liver, but was detected in biliary epithelial cells in the portal area of neonatal and adult livers (Figure 2B). Importantly, Notch2 protein was present only in the biliary epithelial cells that form tubular structures during the remodeling process of the ductal plate, and was absent in the nontubular part of the ductal plate (P1; Figure 2B, c, d). Thus, during

Figure 1. Jagged1 was expressed in the portal mesenchyme adjacent to the developing IHBD in neonatal liver. (A) Jagged1 mRNA expression in the liver by semiquantitative RT-PCR. Jagged1 mRNA was increased at P1 and P7. AFP, α-fetoprotein; α1-AT, α1-antitrypsin. (B) Jagged1 protein distribution by immunohistochemistry at P7. Jagged1 protein was expressed in the portal mesenchyme such as portal veins, hepatic arteries, and periportal connective tissue, but not in the central veins, hepatocytes, or bile ducts. The outlined area in (a) is magnified in (b). (C) Jagged1 protein expression of portal mesenchyme during liver development by immunohistochemistry. Strong staining was observed at ED18.5 and P7 (arrows). (D) Dual immunofluorescence for Jagged1 (red) and keratin (a biliary specific marker, green) at ED18.5 (a) and P7 (b). (a) and (b) are serial liver sections to (C, b) and (C, c), respectively. Jagged1 protein in the portal mesenchyme was predominantly observed adjacent to the biliary epithelial cells during the IHBD development. BD, bile duct; CT, connective tissue; CV, central vein; HA, hepatic artery; PV, portal vein.
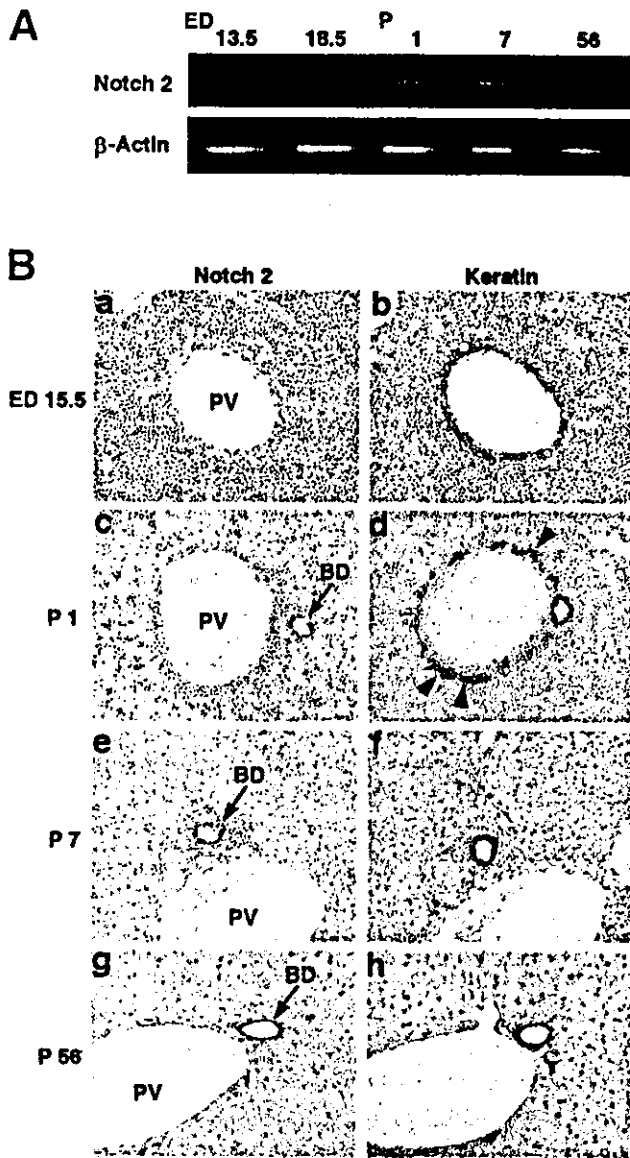
Figure 2. Notch2 was expressed in the biliary epithelial cells that form tubular structures. (A) Notch2 mRNA expression in the liver by semiquantitative RT-PCR. Notch2 mRNA concentration was increased at P1 and P7. (B) Notch2 protein expression and its distribution by immunohistochemistry during liver development (a, c, e, g). Adjacent sections were immunostained with keratin (b, d, f, h, respectively). Notch2 protein was present exclusively in the biliary epithelial cells that form tubular structures (arrows) after birth, although it was absent in the nontubular part of the ductal plate (arrowheads). BD, bile duct; PV, portal vein.

mouse liver development, Notch2 was produced in the tube-forming biliary epithelial cells, and these Notch2-expressing cells were localized adjacent to the Jagged1-expressing cells in the neonatal period. These observations strongly suggest that the Jagged1-expressing portal mesenchyme interacts with Notch2-expressing biliary epithelial cells and affects their development.

Hes1 Expression in the Notch2-Expressing Biliary Epithelial Cells

Next, we examined the expression of Hes1 and Hes5, the major downstream molecules of Notch signaling. In contrast to Hes5 mRNA expression detected mainly in the late fetal period, Hes1 mRNA expression was increased in the neonatal period similar to Jagged1 and Notch2 (Figure 3A). These results suggest that Hes1, but not Hes5, has a role as a downstream Notch signaling gene in neonatal mouse liver. We then investigated Hes1 protein expression during mouse liver development by Western blotting. Hes1 protein concentrations increased during the neonatal period (Figure 3B), confirming the RT-PCR data. Immunohistochemical study revealed that, similar to Jagged1 and Notch2 proteins, Hes1 protein was detected in the portal area of neonatal liver (Figure 3C). Furthermore, similar to Notch2 protein distribution, Hes1 protein was present exclusively in the biliary epithelial cells that form tubular structures, but not in the nontubular part of the ductal plate (Figure 3C, c, d, e, f). In short, Hes1 protein was detected in the nuclei of Notch2-expressing biliary epithelial cells. These observations suggested that, in the portal area of neonatal mouse liver, the Notch2-expressing biliary epithelial cells were activated by Jagged1 and expressed Hes1.

Hepatocyte Differentiation Was Not Impaired in *Hes1* Null Mice

To clarify the role of Hes1 activation in IHBD development further, we analyzed the phenotype of Hes1 null mice liver. Mice homozygous for the Hes1 null mutation died perinatally, and mice heterozygous for the Hes1 null mutation did not exhibit any phenotypes in the liver. We then analyzed the liver of newborn (P0) homozygous mutant mice. First, we analyzed hepatocyte differentiation of Hes1 null mice. Morphologically, the hepatocytes of Hes1 null mice were indistinguishable from those of wild-type mice (H&E staining, data not shown). At a late gestation or perinatal stage, differentiated hepatocytes began to express genes of metabolic enzymes, including α1-antitrypsin, dipeptidylpeptidase IV, tyrosine transaminase, and glucose-6-phosphatase in wild-type mice (Figure 4A), and there was no difference in the gene expressions between Hes1 null mice and wild-type mice at P0 (Figure 4A). On the other hand, hepatocytes were PAS-positive at the perinatal stage in wild-type mice (Figure 4B, a–d). At P0, there was also no difference in the PAS staining level between Hes1 null

mice and wild-type mice (Figure 4*B*, e, f). Thus, the hepatocyte differentiation of *Hes1* null mice was not impaired, at least during the newborn period.
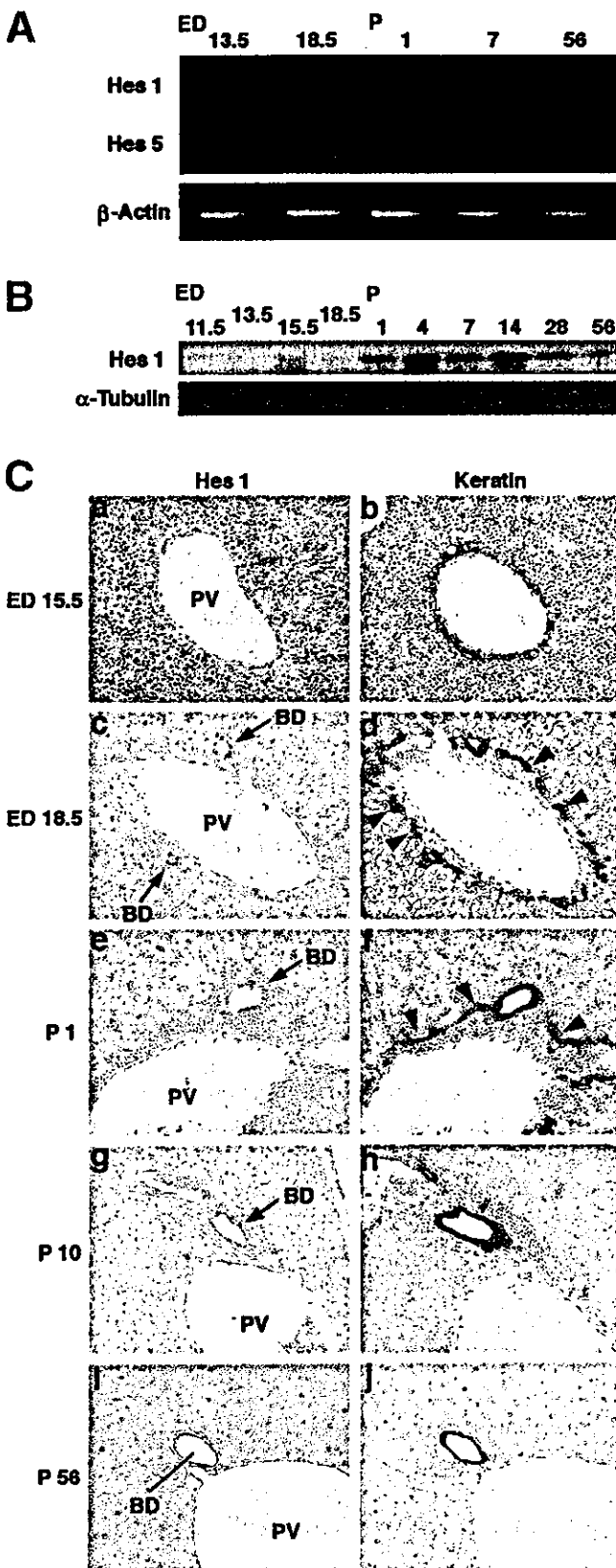
IHBD Development Was Impaired in *Hes1* Null Mice

Next, we analyzed IHBD development of *Hes1* null mice. In wild-type mice, the periportal hepatoblasts started to express keratin at ED13.5. At ED15.5, the biliary epithelial cells began to form the ductal plate; however, these immature biliary epithelial cells did not bind with *Dolichos biflorus* agglutinin (DBA), a bile duct–specific lectin (Figure 5*A*, a, e). At ED18.5, ductal plate remodeling started to form a tubular structure in a part of the ductal plate (Figure 5*A*, f), and during this period, these biliary epithelial cells began to bind with DBA (Figure 5*A*, b). In the neonatal period, the remodeling further progressed to mature the tubular structures and the nontubular part of the ductal plate was eliminated (Figure 5*A*, c, g). Finally, the tubular structures developed into mature bile ducts (Figure 5*A*, d, h). On the other hand, in *Hes1* null mice, the ductal plate formation occurred, consisting of keratin-positive (Figure 5*B*, f–h) and DBA-bound (Figure 5*A*, i, j) biliary epithelial cells. Remarkably, although there were tubular structures in a part of the ductal plate in wild-type mice at P0 (Figure 5*B*, a–d), no such tubular structures were observed in the *Hes1* null mice (Figure 5*B*, e–h). Taken together, in the IHBD development of *Hes1* null mice, although there were no abnormalities in the differentiation of hepatoblasts to biliary epithelial cells, ductal plate formation, and acquisition of the binding ability with DBA, subsequent tubular formation during ductal plate remodeling was blocked completely. These results suggested that Hes1 activation in the developing biliary epithelial cells is essential for their tubular formation. This IHBD phenotype of *Hes1* null mice is very similar to that of mutant mice doubly heterozygous for *Jagged1* and *Notch2*.[14]

Figure 3. Hes1 was expressed in the biliary epithelial cells that form tubular structures during ductal plate remodeling. (*A*) *Hes1* mRNA and *Hes5* mRNA expressions in the liver by semiquantitative RT-PCR. In contrast to *Hes5* mRNA detected in the late fetal period, the *Hes1* mRNA concentration was increased at P1 and P7. (*B*) Hes1 protein expression in the liver by Western blotting. Hes1 protein also increased after birth. (*C*) Hes1 protein expression and its distribution by immunohistochemistry during liver development (a, c, e, g, i). Adjacent sections were immunostained with keratin (b, d, f, h, j, respectively). Hes1 protein was observed exclusively in the biliary epithelial cells that form tubular structures during the ductal plate remodeling between ED18.5 and P10 (*arrows*), whereas it was absent in the nontubular part of the ductal plate (*arrowheads*). BD, bile duct; PV, portal vein.
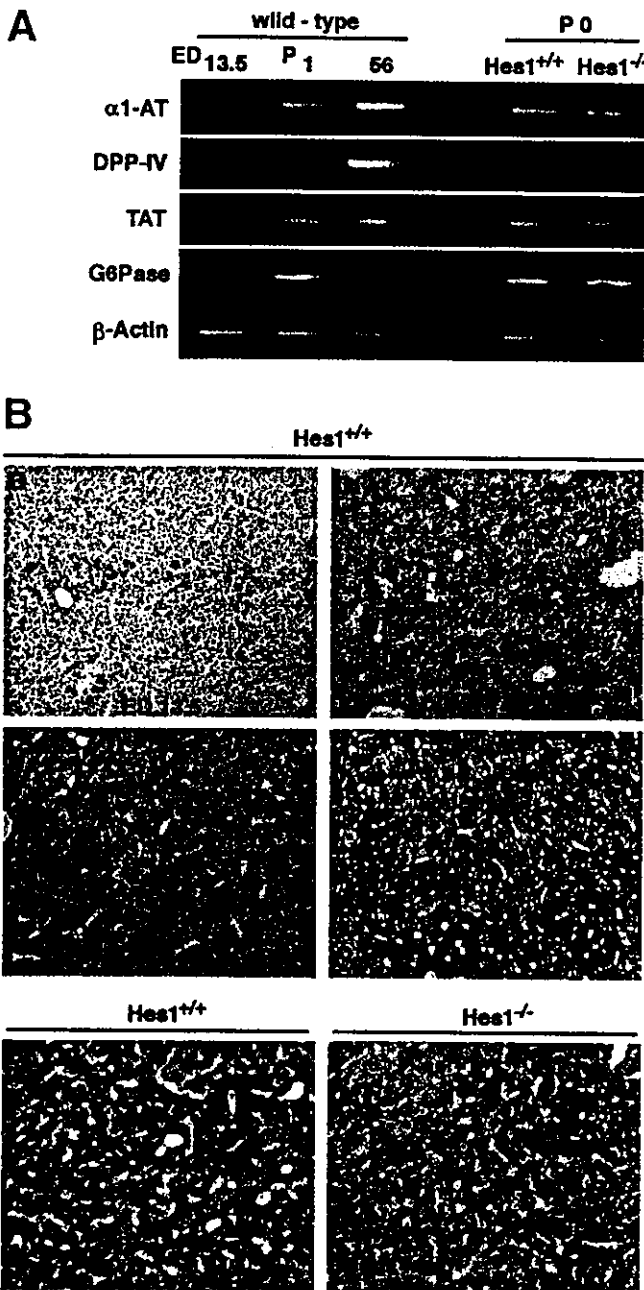
Figure 4. Hepatocyte differentiation was not impaired in *Hes1* null mice. (*A*) The mRNA expression of metabolic enzymes such as α1-antitrypsin, dipeptidylpeptidase IV, tyrosine transaminase, and glucose-6-phosphatase in wild-type mice and *Hes1* null mice by semi-quantitative RT-PCR. In wild-type mice, hepatocytes started to express mRNAs of these enzymes during the perinatal period. Compared with wild-type mice, equal amounts of mRNAs were expressed in *Hes1* null mice at P0. (*B*) PAS staining in wild-type mice and *Hes1* null mice. In wild-type mice, hepatocytes began to be stained with PAS solution during the perinatal period (a–d). At P0, there was no difference in the PAS staining level between *Hes1* null mice and wild-type mice (e, f).

Jagged1 Promoted the Biliary Differentiation of WB-F344 Cells

An in vitro 2-cell coculture assay system was used to clarify the role of Notch signaling in the differentia-

tion of biliary epithelial cells. The WB-F344 cell line, derived from normal adult rat liver,[26] is considered to be a culture counterpart of bipotential liver precursor cells that can differentiate into both hepatocyte and biliary lineages.[27–29] After we confirmed the expression of Notch2 on WB-F344 cells (data not shown), we investigated the effect of Jagged1 in WB-F344 cells by coculture with Jagged1-expressing Balb3T3 cells.

First, we confirmed that Jagged1 protein was expressed only on the membrane of *Jagged1*-transfected Balb3T3 cells (Balb3T3 Jagged1), but not on control cells (Balb3T3 control) (Figure 6A). Then we examined whether Notch signaling in WB-F344 cells is activated by coculture with Balb3T3 Jagged1 cells. WB-F344 cells were transfected with the luciferase reporter plasmid under the control of the *Hes1* promoter, and cocultured with either Balb3T3 control or Balb3T3 Jagged1 cells. The *Hes1* promoter was activated when cocultured with Balb3T3 Jagged1 cells, but not with Balb3T3 control cells (Figure 6B, left). This transactivation was not observed when the 2 cells were separated by a transwell membrane (Figure 6B, right), suggesting that Notch signaling activation in WB-F344 cells is dependent on contact with Balb3T3 Jagged1 cells and was not mediated by a soluble factor from Balb3T3 cells. Hes1 protein also was up-regulated only when cocultured in contact with Balb3T3 Jagged1 cells (Figure 6C).

After culturing WB-F344 cells for 3 days either with Balb3T3 control or Balb3T3 Jagged1 cells, the expression of several hepatocyte or biliary lineage marker genes was analyzed by real-time quantitative RT-PCR. When WB-F344 cells were cocultured with Balb3T3 Jagged1 cells, expression of albumin mRNA, a hepatocyte lineage marker, was decreased compared with that of Balb3T3 control cells (Figure 6D, left). By contrast, WB-F344 cells exhibited a several-fold increase in mRNA expression of biliary lineage markers such as cytokeratin-19 and γ-glutamyl transpeptidase by coculture with Balb3T3 Jagged1 cells as compared with Balb3T3 control cells (Figure 6D, middle, right). Thus, Jagged1-activated Notch signaling in WB-F344 cells promotes their biliary differentiation and inhibits their differentiation toward hepatocytes.

Discussion

Since *Jagged1* was identified as the gene responsible for AGS in 1997, it has been thought that Notch signaling has an important role in IHBD development. Previous genetic and pathologic studies on AGS indicate that the bile duct paucity in AGS is caused by impaired postnatal development of IHBD. To date, however, it is
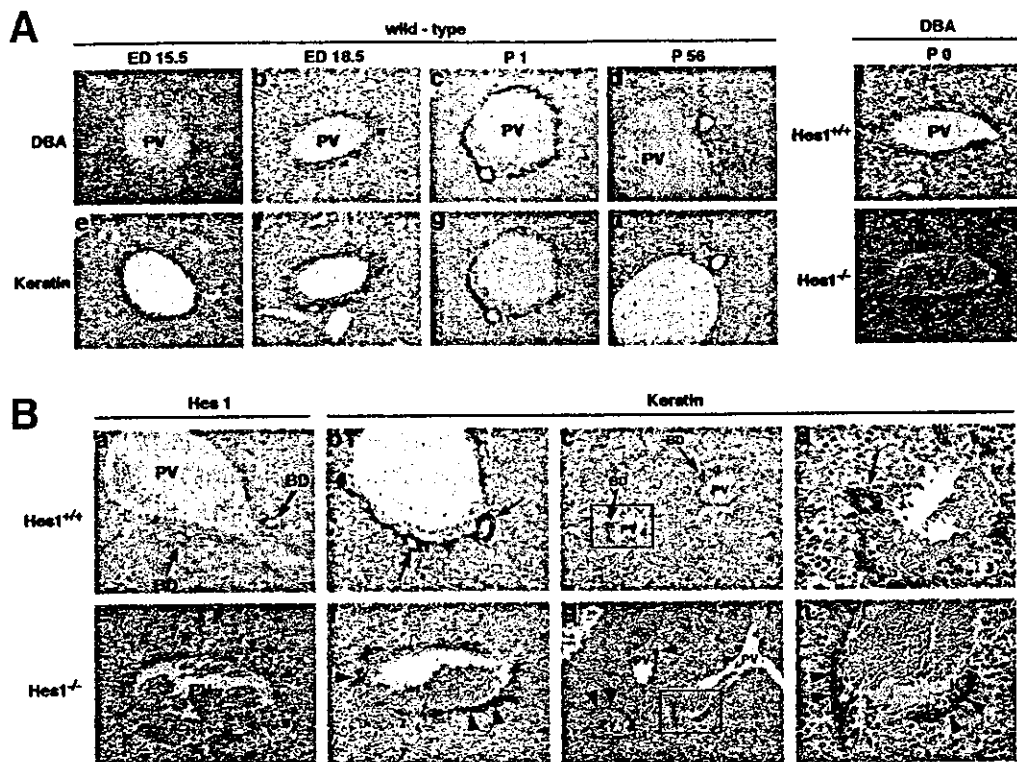
Figure 5. IHBD development was impaired in *Hes1* null mice. (*A*) DBA binding of biliary epithelial cells in wild-type and *Hes1* null mice. DBA staining was performed serially in wild-type mice liver sections (a–d). Adjacent sections were immunostained with keratin (e–h, respectively). In wild-type mice, biliary epithelial cells were able to bind with DBA at the perinatal period (b, c). The DBA binding of biliary epithelial cells was not different between *Hes1* null and wild-type mice at P0 (i, j). (*B*) IHBD development in *Hes1* null mice in comparison with wild-type mice at P0. Hes1 protein was immunostained in *Hes1*^{+/+} (a) or *Hes1*^{−/−} mice (e). IHBD development was analyzed by keratin immunohistochemistry in *Hes1*^{+/+} (b–d) or *Hes1*^{−/−} mice (f–h). (b) and (f) were serial sections to (a) and (e), respectively. The *outlined* area in (c) and (g) is magnified in (d) and (h), respectively. There were tubular structures (*arrows*) that expressed Hes1 protein in a part of the ductal plate in wild-type mice (a–d), whereas in *Hes1* null mice, no such tubular structures were observed, although there was the ductal plate formation (*arrowheads*) (e–h). BD, bile duct; PV, portal vein.

not known which lineage cells in the liver express Jagged1 and Notch, when and where they interact with each other, and what the precise role for Notch signaling is in IHBD development. The present study showed that the Notch signaling pathway, consisting of Jagged1, Notch2, and Hes1, is activated by the interaction between the periportal mesenchyme and biliary epithelial cells in the neonatal liver.

Findings in mice heterozygous for the *Jagged1* mutation[13] and mice doubly heterozygous for the *Jagged1* and *Notch2* mutation[14] suggest that interactions between Jagged1 and Notch2 have an important role in mouse IHBD development. Thus, we analyzed the expression and distribution patterns of Jagged1 and Notch2 during liver development. Although there have been several studies on Jagged1 expression in the liver, these results are still in controversy.[14,30–34] In our present study, consistent with the reports by Jones et al,[31] Crosnier et al,[32] or McCright et al,[14] Jagged1 was expressed only in portal vein and hepatic artery, but neither in ductal plate nor bile duct cells throughout the entire period from

fetus to adult. Furthermore, as previously reported,[35] Jagged1 was present not only in the endothelial cells of portal veins and hepatic arteries, but also in the arterial smooth muscle cells and periportal connective tissues. In addition, during liver development, Jagged1 expression in the portal mesenchyme becomes most remarkable in the neonatal period, suggesting that Jagged1 is functioning in this period. On the other hand, there have been few studies of Notch2 expression in the liver.[14,34,36] In the present study, Notch2 was expressed in the developing biliary epithelial cells in the portal area after birth. This result is consistent with the previous report by Nijjar et al[36] showing that Notch2 is expressed in adult human bile ducts. Although McCright et al[14] failed to find Notch2 in bile ducts, they proposed that at least some of the Notch2-expressing cells were biliary lineage cells. It should be emphasized that in our study, Notch2-expressing biliary epithelial cells were observed predominantly in the vicinity of Jagged1-expressing portal mesenchyme. Previous in vitro studies showed that Jagged1 physically interacts with Notch2 and activates the tran
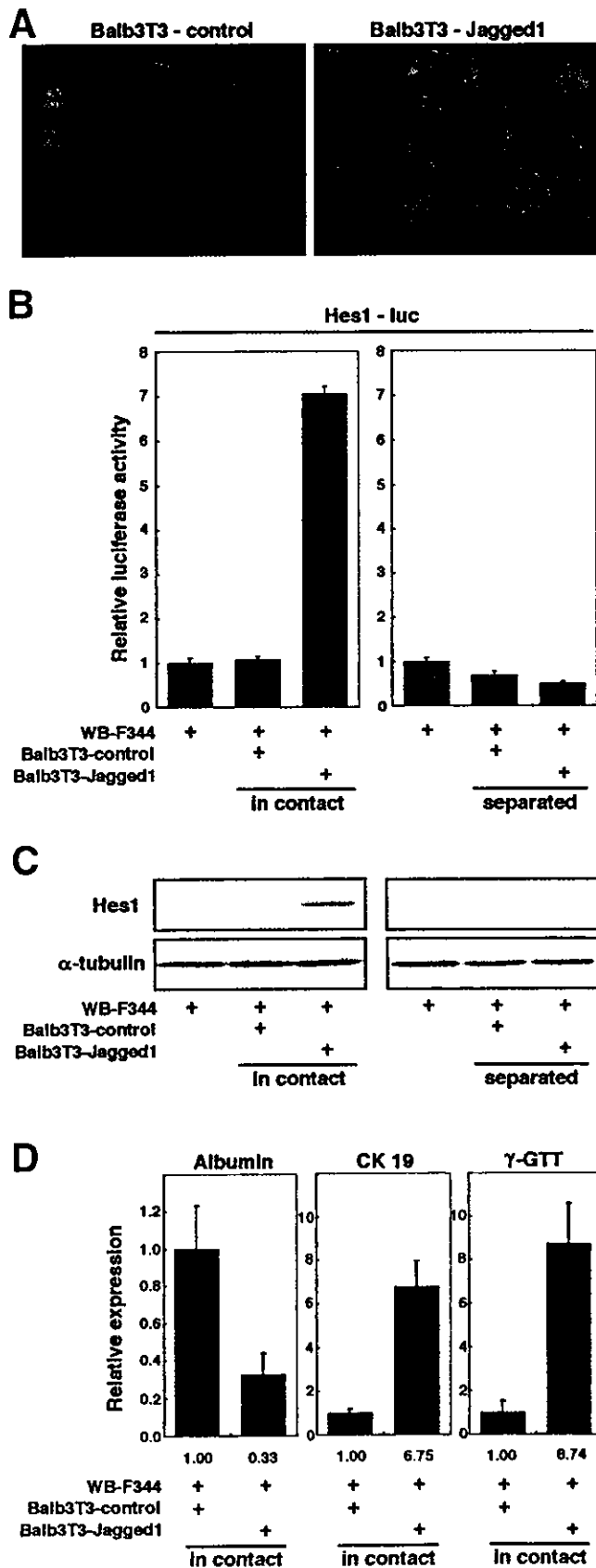
scription of their downstream genes.[37,38] Thus, our data strongly suggest that, in the neonatal liver, Jagged1 in the portal mesenchyme interacts with Notch2 in the developing biliary epithelial cells adjacent to Jagged1-expressing mesenchyme. To confirm this, we analyzed the expression of Hes1, a major downstream molecule of Notch signaling. Sumazaki et al[39] recently showed that Hes1 is expressed in the extrahepatic biliary epithelium and is essential for its development. Here, we show that Hes1 is expressed in the Notch2-expressing biliary epithelial cells in the liver, suggesting activation of the Notch signaling in the developing biliary epithelial cells. Thus, it appears that Jagged1-Notch2 interactions in the neonatal portal area activate Hes1 in the developing biliary epithelial cells and influence their differentiation. This model is supported by the findings that the IHBD phenotype of Hes1 null mice is very similar to that of mice doubly heterozygous for the Jagged1 and Notch2 mutation.[11]

What is the precise role of Notch signaling activation in biliary epithelial cell development? As stated earlier, mammalian IHBD development can be divided into several stages: lineage commitment stage from hepatoblast to biliary epithelial cells, ductal plate formation stage, ductal plate remodeling stage, and bile duct maturation stage. In our study, Notch2 and Hes1 were detected in the neonatal biliary epithelial cells during

Figure 6. Jagged1 induced Notch signaling activation in WB-F344 cells and promoted their biliary differentiation. (A) Membrane localization of Jagged1 by immunofluorescence in the cell lines. Jagged1 protein (red) was expressed strongly only in Balb3T3 Jagged1 cells. Nuclear staining of cells was performed using 4',6-diamidino-2-phenylindole dihydrochloride (blue). (B) Hes1 promoter transactivation in WB-F344 cells by Jagged1. WB-F344 cells were transfected transiently with Hes1 reporter plasmid. Twelve hours later, either no cells, Balb3T3 control cells, or Balb3T3 Jagged1 cells were added. Two cells were cocultured in contact with each other (without a transwell membrane between the 2 cells, left panel) or separated (with a transwell membrane, right panel) from each other. Luciferase activation represents the ratio between individual luciferase activity and the activity measured with the reporter plasmid alone. The data are means ± SE from 3 independent experiments. Hes1 promoter was activated in WB-F344 cells only when cocultured in contact with Balb3T3 Jagged1 cells. (C) Hes1 protein production in WB-F344 cells by Jagged1. Two-cell coculture was performed as described earlier. Hes1 protein was produced only when cocultured in contact with Balb3T3 Jagged1 cells. (D) Hepatocyte or biliary differentiation of WB-F344 cells by Jagged1 assessed by real-time quantitative RT-PCR. WB-F344 cells were cocultured in contact with Balb3T3 Jagged1 cells or Balb3T3 control cells for 3 days. All expression levels are normalized to the 18S ribosomal RNA levels and represent the ratio between coculture with Balb3T3 Jagged1 cells and Balb3T3 control cells. The data are means ± SE from 3 independent experiments. Compared with control, Jagged1 decreased albumin expression. In contrast, Jagged1 induced the expression of biliary lineage markers such as cytokeratin-19 and γ-glutamyl transpeptidase.

ductal plate remodeling to the bile duct maturation stage. Interestingly, both Notch2 and Hes1 were present exclusively in the biliary epithelial cells that form tubular structures, but absent in the nontubular part of the ductal plate. This report shows the difference between the tubular part and nontubular part of the ductal plate. Moreover, these results strongly suggest that Notch signaling activation in the biliary epithelial cells is an important factor in tubular formation and maturation, namely ductal plate remodeling. In fact, similar to the mice doubly heterozygous for the *Jagged1* and *Notch2* mutation reported by McCright et al,[14] no patent bile ducts or tubular structures consisting of biliary epithelial cells were present in the liver of *Hes1* null mice, although their biliary commitment or ductal plate formation were not impaired.

In this study, we further supported our in vivo findings by using the in vitro 2-cell coculture assay system. We showed that Jagged1-expressing fibroblasts activated Notch signaling and induced biliary differentiation in WB-F344 cells, and this differentiation was observed only when WB-F344 cells were in contact with Jagged1-expressing cells. Although we failed to induce bile duct formation in vitro, these experiments mimicked biliary epithelial cell differentiation by contacting the portal mesenchyme. These findings further suggested that Notch signaling activation induced by mesenchymal Jagged1 has an important role in biliary epithelial cell differentiation.

Similar to our observations, it has been reported that in humans the ductal plate remodeling and bile duct maturation also progress in the late fetal to neonatal period.[40,41] Thus, our present data are consistent with the idea that, in AGS, insufficient activation of Notch signaling in the biliary epithelial cells owing to *Jagged1* mutation is a principal cause of impaired ductal plate remodeling and subsequent impaired postnatal IHBD development. In this regard, *Hes1* null mice appear to be a good model for AGS in their IHBD phenotype. Besides paucity of IHBD, AGS patients exhibit other features such as eye abnormalities, vertebral anomalies, congenital heart defects, kidney abnormalities, and a characteristic facial appearance. Among them, phenotypes of liver, eye, heart, and kidney were reproduced in mice doubly heterozygous for the *Jagged1* and *Notch2* mutation.[14] In *Hes1* null mice, in addition to our present findings of impaired IHBD development, the eye abnormalities have been shown previously.[42,43] In contrast, it was reported that these mutant mice do not display vertebral defects.[18,44] Furthermore, although we intensively investigated the *Hes1* null mice in this study, no abnormalities were found in their heart, kidney, and craniofacial de-

velopment (data not shown). Consequently, the phenotypes of the mice doubly heterozygous for the *Jagged1* and *Notch2* mutation were reproduced only in liver and eye of *Hes1* null mice. These findings suggest that Hes1 plays a crucial role as the downstream target for Jagged1 and Notch2, especially in liver and eye development. Although the precise reason for the phenotypic difference between *Hes1* null mice and mice doubly heterozygous for the *Jagged1* and *Notch2* mutation is unclear at present, it is possible that in the heart and kidney of *Hes1* null mice, the deficiency of *Hes1* is compensated by some other target genes of Notch signaling pathway such as *Hey* genes, that recently were reported to be essential for cardiovascular development[45–47] and to be expressed in the developing kidney.[48]

In summary, our data show that Notch signaling is activated through epithelial-mesenchymal interactions during IHBD development, and is essential for the control of ductal plate remodeling and bile duct maturation. Besides AGS, various congenital diseases of IHBD have been considered to originate from abnormalities in ductal plate remodeling, so-called ductal plate malformation.[49,50] Furthermore, recent studies suggested the possible contribution of Notch signaling to biliary defects in adult human diseased liver.[33,36] Thus, further studies are required to clarify the precise role of Notch signaling not only in IHBD development but also in the pathogenesis of various congenital or acquired biliary diseases.

References

1. Artavanis-Tsakonas S, Rand MD, Lake RJ. Notch signaling: cell fate control and signal integration in development. Science 1999; 284:770–776.
2. Li L, Krantz ID, Deng Y, Genin A, Banta AB, Collins CC, Qi M, Trask BJ, Kuo WL, Cochran J, Costa T, Pierpont ME, Rand EB, Piccoli DA, Hood L, Spinner NB. Alagille syndrome is caused by mutations in human Jagged1, which encodes a ligand for Notch1. Nat Genet 1997;16:243–251.
3. Oda T, Elkahloun AG, Pike BL, Okajima K, Krantz ID, Genin A, Piccoli DA, Meltzer PS, Spinner NB, Collins FS, Chandrasekharappa SC. Mutations in the human Jagged1 gene are responsible for Alagille syndrome. Nat Genet 1997;16:235–242.
4. Alagille D, Estrada A, Hadchouel M, Gautier M, Odievre M, Dommergues JP. Syndromic paucity of interlobular bile ducts (Alagille syndrome or arteriohepatic dysplasia): review of 80 cases. J Pediatr 1987;110:195–200.
5. Krantz ID, Piccoli DA, Spinner NB. Alagille syndrome. J Med Genet 1997;34:152–157.
6. Emerick KM, Rand EB, Goldmuntz E, Krantz ID, Spinner NB, Piccoli DA. Features of Alagille syndrome in 92 patients: frequency and relation to prognosis. Hepatology 1999;29:822–829.
7. Krantz ID, Colliton RP, Genin A, Rand EB, Li L, Piccoli DA, Spinner NB. Spectrum and frequency of jagged1 (JAG1) mutations in Alagille syndrome patients and their families. Am J Hum Genet 1998;62:1361–1369.
8. Crosnier C, Driancourt C, Raynaud N, Dhorne-Pollet S, Pollet N, Bernard O, Hadchouel M, Meunier-Rotival M. Mutations in

JAGGED1 gene are predominantly sporadic in Alagille syndrome. Gastroenterology 1999;116:1141–1148.

9. Colliton RP, Bason L, Lu FM, Piccoli DA, Krantz ID, Spinner NB. Mutation analysis of Jagged1 (JAG1) in Alagille syndrome patients. Hum Mutat 2001;17:151–152.

10. Spinner NB, Colliton RP, Crosnier C, Krantz ID, Hadchouel M, Meunier-Rotival M. Jagged1 mutations in Alagille syndrome. Hum Mutat 2001;17:18–33.

11. Quiros-Tejeira RE, Ament ME, Heyman MB, Martin MG, Rosenthal P, Hall TR, McDiarmid SV, Vargas JH. Variable morbidity in Alagille syndrome: a review of 43 cases. J Pediatr Gastroenterol Nutr 1999;29:431–437.

12. Piccoli DA, Spinner NB. Alagille syndrome and the Jagged1 gene. Semin Liver Dis 2001;21:525–534.

13. Xue Y, Gao X, Lindsell CE, Norton CR, Chang B, Hicks C, Gendron-Maguire M, Rand EB, Weinmaster G, Gridley T. Embryonic lethality and vascular defects in mice lacking the Notch ligand Jagged1. Hum Mol Genet 1999;8:723–730.

14. McCright B, Lozier J, Gridley T. A mouse model of Alagille syndrome: Notch2 as a genetic modifier of Jag1 haploinsufficiency. Development 2002;129:1075–1082.

15. Shiojiri N. The origin of intrahepatic bile duct cells in the mouse. J Embryol Exp Morphol 1984;79:25–39.

16. Germain L, Blouin MJ, Marceau N. Biliary epithelial and hepatocytic cell lineage relationships in embryonic rat liver as determined by the differential expression of cytokeratins, alpha-fetoprotein, albumin, and cell surface-exposed components. Cancer Res 1988;48:4909–4918.

17. Van Eyken P, Sciot R, Callea F, Van der Steen K, Moerman P, Desmet VJ. The development of the intrahepatic bile ducts in man: a keratin-immunohistochemical study. Hepatology 1988;8:1586–1595.

18. Ishibashi M, Ang SL, Shiota K, Nakanishi S, Kageyama R, Guillemot F. Targeted disruption of mammalian hairy and Enhancer of split homolog-1 (HES-1) leads to up-regulation of neural helix-loop-helix factors, premature neurogenesis, and severe neural tube defects. Genes Dev 1995;9:3136–3148.

19. Karanu FN, Murdoch B, Gallacher L, Wu DM, Koremoto M, Sakano S, Bhatia M. The notch ligand jagged-1 represents a novel growth factor of human hematopoietic stem cells. J Exp Med 2000;192:1365–1372.

20. Iwai A, Marusawa H, Kiuchi T, Higashitsuji H, Tanaka K, Fujita J, Chiba T. Role of a novel oncogenic protein, gankyrin, in hepatocyte proliferation. J Gastroenterol 2003;38:751–758.

21. Hijikata M, Mizushima H, Akagi T, Mori S, Kakiuchi N, Kato N, Tanaka T, Kimura K, Shimotohno K. Two distinct proteinase activities required for the processing of a putative nonstructural precursor protein of hepatitis C virus. J Virol 1993;67:4665–4675.

22. Ito T, Udaka N, Yazawa T, Okudela K, Hayashi H, Sudo T, Guillemot F, Kageyama R, Kitamura H. Basic helix-loop-helix transcription factors regulate the neuroendocrine differentiation of fetal mouse pulmonary epithelium. Development 2000;127:3913–3921.

23. Nettleton GS, Carpenter AM. Studies of the mechanism of the periodic acid-Schiff histochemical reaction for glycogen using infrared spectroscopy and model chemical compounds. Stain Technol 1977;52:63–77.

24. Kuroda K, Tani S, Tamura K, Minoguchi S, Kurooka H, Honjo T. Delta-induced Notch signaling mediated by RBP-J inhibits MyoD expression and myogenesis. J Biol Chem 1999;274:7238–7244.

25. Takagi S, Ueda Y, Hijikata M, Shimotohno K. Overproduced p73alpha activates a minimal promoter through a mechanism independent of its transcriptional activity. FEBS Lett 2001;509:47–52.

26. Tsao MS, Smith JD, Nelson KG, Grisham JW. A diploid epithelial cell line from normal adult rat liver with phenotypic properties of 'oval' cells. Exp Cell Res 1984;154:38–52.

27. Tsao MS, Grisham JW. Hepatocarcinomas, cholangiocarcinomas, and hepatoblastomas produced by chemically transformed cultured rat liver epithelial cells. A light- and electron-microscopic analysis. Am J Pathol 1987;127:168–181.

28. Grisham JW, Coleman WB, Smith GJ. Isolation, culture, and transplantation of rat hepatocytic precursor (stem-like) cells. Proc Soc Exp Biol Med 1993;204:270–279.

29. Coleman WB, McCullough KD, Esch GL, Faris RA, Hixson DC, Smith GJ, Grisham JW. Evaluation of the differentiation potential of WB-F344 rat liver epithelial stem-like cells in vivo. Differentiation to hepatocytes after transplantation into dipeptidylpeptidase-IV-deficient rat liver. Am J Pathol 1997;151:353–359.

30. Louis AA, Van Eyken P, Haber BA, Hicks C, Weinmaster G, Taub R, Rand EB. Hepatic jagged1 expression studies. Hepatology 1999;30:1269–1275.

31. Jones EA, Clement-Jones M, Wilson DI. JAGGED1 expression in human embryos: correlation with the Alagille syndrome phenotype. J Med Genet 2000;37:663–668.

32. Crosnier C, Attie-Bitach T, Encha-Razavi F, Audollent S, Soudy F, Hadchouel M, Meunier-Rotival M, Vekemans M. JAGGED1 gene expression during human embryogenesis elucidates the wide phenotypic spectrum of Alagille syndrome. Hepatology 2000;32:574–581.

33. Nijjar SS, Wallace L, Crosby HA, Hubscher SG, Strain AJ. Altered Notch ligand expression in human liver disease: further evidence for a role of the Notch signaling pathway in hepatic neovascularization and biliary ductular defects. Am J Pathol 2002;160:1695–1703.

34. Loomes KM, Taichman DB, Glover CL, Williams PT, Markowitz JE, Piccoli DA, Baldwin HS, Oakey RJ. Characterization of Notch receptor expression in the developing mammalian heart and liver. Am J Med Genet 2002;112:181–189.

35. Villa N, Walker L, Lindsell CE, Gasson J, Iruela-Arispe ML, Weinmaster G. Vascular expression of Notch pathway receptors and ligands is restricted to arterial vessels. Mech Dev 2001;108:161–164.

36. Nijjar SS, Crosby HA, Wallace L, Hubscher SG, Strain AJ. Notch receptor expression in adult human liver: a possible role in bile duct formation and hepatic neovascularization. Hepatology 2001;34:1184–1192.

37. Shimizu K, Chiba S, Kumano K, Hosoya N, Takahashi T, Kanda Y, Hamada Y, Yazaki Y, Hirai H. Mouse jagged1 physically interacts with notch2 and other notch receptors. Assessment by quantitative methods. J Biol Chem 1999;274:32961–32969.

38. Shimizu K, Chiba S, Hosoya N, Kumano K, Saito T, Kurokawa M, Kanda Y, Hamada Y, Hirai H. Binding of Delta1, Jagged1, and Jagged2 to Notch2 rapidly induces cleavage, nuclear translocation, and hyperphosphorylation of Notch2. Mol Cell Biol 2000;20:6913–6922.

39. Sumazaki R, Shiojiri N, Isoyama S, Masu M, Keino-Masu K, Osawa M, Nakauchi H, Kageyama R, Matsui A. Conversion of biliary system to pancreatic tissue in Hes1-deficient mice. Nat Genet 2004;36:83–87.

40. Terada T, Nakanuma Y. Profiles of expression of carbohydrate chain structures during human intrahepatic bile duct development and maturation: a lectin-histochemical and immunohistochemical study. Hepatology 1994;20:388–397.

41. Nakanuma Y, Hoso M, Sanzen T, Sasaki M. Microstructure and development of the normal and pathologic biliary tract in humans, including blood supply. Microsc Res Tech 1997;38:552–570.

42. Tomita K, Ishibashi M, Nakahara K, Ang SL, Nakanishi S, Guillemot F, Kageyama R. Mammalian hairy and enhancer of split homolog 1 regulates differentiation of retinal neurons and is essential for eye morphogenesis. Neuron 1996;16:723–734.

43. Takatsuka K, Hatakeyama J, Bessho Y, Kageyama R. Roles of the bHLH gene Hes1 in retinal morphogenesis. Brain Res 2004; 1004:148–155.

44. Jouve C, Palmeirim I, Henrique D, Beckers J, Gossler A, Ish-Horowicz D, Pourquie O. Notch signalling is required for cyclic expression of the hairy-like gene HES1 in the presomitic mesoderm. Development 2000;127:1421–1429.

45. Gessler M, Knobeloch KP, Helisch A, Amann K, Schumacher N, Rohde E, Fischer A, Leimeister C. Mouse gridlock: no aortic coarctation or deficiency, but fatal cardiac defects in Hey2−/− mice. Curr Biol 2002;12:1601–1604.

46. Donovan J, Kordylewska A, Jan YN, Utset MF. Tetralogy of Fallot and other congenital heart defects in Hey2 mutant mice. Curr Biol 2002;12:1605–1610.

47. Sakata Y, Kamei CN, Nakagami H, Bronson R, Liao JK, Chin MT. Ventricular septal defect and cardiomyopathy in mice lacking the transcription factor CHF1/Hey2. Proc Natl Acad Sci U S A 2002; 99:16197–16202.

48. Leimeister C, Schumacher N, Gessler M. Expression of Notch pathway genes in the embryonic mouse metanephros suggests a role in proximal tubule development. Gene Expr Patterns 2003;3:595–598.

49. Desmet VJ. Congenital diseases of intrahepatic bile ducts: variations on the theme "ductal plate malformation." Hepatology 1992;16:1069–1083.

50. Desmet VJ. Ludwig symposium on biliary disorders—part I. Pathogenesis of ductal plate abnormalities. Mayo Clin Proc 1998;73:80–89.

VIROLOGY

ELSEVIER

Suppression of hepatitis C virus replicon by TGF-β

Takayuki Murata, Takayuki Ohshima, Masashi Yamaji, Masahiro Hosaka, Yusuke Miyanari, Makoto Hijikata, Kunitada Shimotohno*

Department of Viral Oncology, Institute for Virus Research, Kyoto University, Sakyo-ku, Kyoto 606-8507, Japan

Abstract

Hepatitis C virus (HCV) is one of the major causative agents of liver diseases, such as liver inflammation, fibrosis, cirrhosis, and hepatocellular carcinoma. Using an efficient HCV subgenomic replicon system, we demonstrate that transforming growth factor-beta (TGF-β) suppresses viral RNA replication and protein expression from the HCV replicon. We further show that the anti-viral effect of this cytokine is associated with cellular growth arrest in a manner dependent on Smad signaling, not mitogen-activated protein kinase (MAPK) signaling. These results suggest a novel insight into the mechanisms of liver diseases caused by HCV.
© 2004 Elsevier Inc. All rights reserved.

Keywords: TGF-β; Hepatitis C virus; Replicon; Smad; MAPK

Introduction

Hepatitis C virus (HCV), a member of the *Flaviviridae* family, is an enveloped virus with a positive single-stranded 9.6-kb RNA genome (Murphy et al., 1995). The virus has been identified as the major causative agent of non-A, non-B hepatitis (Choo et al., 1989) that persistently infects several millions of people throughout the world. Although acute phase HCV infection is asymptomatic in most cases, the virus frequently establishes a persistent infection. This condition is associated with serious clinical diseases, including chronic hepatitis and liver fibrosis, which can lead to liver cirrhosis and eventually hepatocellular carcinoma (Goodman and Ishak, 1995).

Despite the clinical significance, molecular investigation of the virus has been hampered due to the lack of cell culture systems that efficiently support HCV replication. In 1999, the establishment of an HCV subgenomic replicon cell culture system (Lohmann et al., 1999) improved the situation. The subgenomic replicon RNA is composed of the HCV 5′-untranslated region (UTR) containing an

internal ribosomal entry site (IRES), a neomycin phosphotransferase (*neo*) gene, the HCV nonstructural (NS) proteins 3 through 5B under the control of an encephalomyocarditis virus (EMCV) IRES, followed by the HCV 3′-UTR. The *neo* gene is expressed under the control of the HCV IRES, and thereby, gives the resistance to the cells in which replicon RNA exists. Instead of the *neo* gene, the luciferase gene can be used as a marker. Using the luciferase gene is beneficial in that it offers easy, speedy, and reliable detection. As the RNA replicates autonomously in cultured cells, this replicon system provides a unique tool for the analysis of the molecular mechanisms of HCV replication and the screening of anti-HCV compounds.

Transforming growth factor-beta (TGF-β) promotes the development of liver fibrosis and cirrhosis (Gressner et al., 2002); serum cytokine levels are associated with the severity of liver fibrosis in patients with chronic HCV (Nelson et al., 1997; Neuman et al., 2001; Tsushima et al., 1999). As high levels of TGF-β expression correlate with chronic hepatitis and cirrhosis (Calabrese et al., 2003; Shirai et al., 1994), cytokine serum concentrations serve as useful serologic markers for hepatitis, cirrhosis, and carcinoma (Song et al., 2002). Despite accumulating clinical observations, the direct effect of TGF-β on HCV replication remains unknown.

* Corresponding author. Fax: +81 75 751 3998.
E-mail address: kshimoto@virus.kyoto-u.ac.jp (K. Shimotohno).

Molecular biological analyses have revealed that the cytokine is a multifunctional cytokine that regulates multiple biological functions, including cellular growth inhibition, extracellular matrix (ECM) formation, apoptosis, and cell differentiation (reviewed in Derynck and Zhang, 2003; Miyazono et al., 2000). Following receptor ligation, the activation of receptor-regulated Smad (R-Smad, Smad2, and Smad3) enhances complex formation with the common-mediator Smad (Co-Smad, Smad4). These complexes translocate to the nucleus, where they directly regulate the transcription of various target genes. TGF-β receptor ligation also activates members of the mitogen-activated protein kinase (MAPK) family, including p38 MAPK, c-Jun N-terminal kinase (JNK), and extracellular signal-regulated kinase (ERK).

In this study, we demonstrate that TGF-β inhibits HCV RNA replication and viral protein expression using a HCV subgenomic replicon system. The anti-viral effect of TGF-β was associated with growth arrest of cells and the activation of Smad, not MAPK, signaling. Our results provide insight into the mechanisms of liver disease pathogenesis caused by HCV.

Results

Construction of a highly efficient and sensitive replicon system

Although we had previously developed subgenomic HCV replicon cell lines (Kishine et al., 2002), we desired a highly efficient replicon system to study the molecular mechanisms of HCV replication. Among the G418-resistant subgenomic replicon cell lines, we identified a replicon cell clone (MH14) in which the viral RNA levels were higher than those in other replicon cells (Miyanari et al., 2003). The amount of replicon RNA present in MH14 cells was approximately five times greater than that present in typical MH5 replicon cells (Fig. 1B). The production of NS5A protein in MH14 cells was also greater (Fig. 1C), suggesting efficient replication of the viral RNA. Sequence analysis of replicon RNA in the MH14 cells revealed two point mutations; S2204R, the replacement of the Ser residue at position 2204 with Arg, and a silent mutation L1882L in the NS4B coding region, which did not encode an amino acid substitution. The S2204R mutation corresponded to a previously reported adaptive mutation in NS5A (Lohmann et al., 2003). At least two forms of NS5A, p56 (basally phosphorylated form), and p58 (hyper-phosphory-lated form), have been reported. Residue Ser-2204 is important for hyper-phosphorylation of the protein (Tanji et al., 1995). As expected, only the basally phosphorylated p56 form was detected and hyper-phosphorylated p58 was missing in the MH14 cells, while MH5 cells, which do not carry a mutation at the sequences liable for the hyper-phosphorylation, produce both the p56 and p58 forms of NS5A (Fig. 1C).

To test permissiveness of MH14 cells for HCV replication, cells were cured of the HCV replicon RNA by prolonged treatment with IFN-α, resulting in the curedMH14 line (Figs. 1B, C). MH5 replicon cells were treated with IFN-α in parallel, for use as controls. To examine permissiveness, cured cells were transfected with replicon RNAs in which the firefly luciferase gene was inserted (Fig. 1A). We, here, used luciferase gene as a marker since it is more convenient and has the sensitivity for better quantitation. Cells were harvested at various time points after transfection and cellular luciferase activities were measured subsequently (Figs. 1D–F). Luciferase activity in transfected cells reflects the replication of the replicon RNA. Polymerase-defective RNA replicon constructs, in which the catalytic GDD motif of the NS5B polymerase was substituted to the inactive GHD motif, were used as negative controls. When cells were transfected with the prototype NN replicon RNA, luciferase activity decreased rapidly 3 to 5 days after transfection (Figs. 1D–F, NN). Use of the MH14 RNA, which is identical to the prototype NN RNA with the exception of the L1882L and S2204R mutations, resulted in higher luciferase activities (Figs. 1D–F, MH14) than those observed in cells transfected with the NN RNA. For the curedMH14 cells, luciferase activity did not decrease (Fig. 1F, MH14), but increased, peaking 3 to 5 days after transfection, suggesting highly efficient replication.

We also tested the effect of the mutations and cured cell lines on G418-resistance transduction efficiencies (not shown) and confirmed that the numbers of G418-resistant colonies exhibited a similar trend as seen for the luciferase activities described above.

These results suggest that the curedMH14 cells were highly permissive for replication of RNA containing the adaptive mutations.

Furthermore, when curedMH14 cells were transfected with the highest efficiency replicon RNA, high luciferase activity persisted for greater than 1 month (data not shown) in the absence of selection.

Suppression of HCV replicon with luciferase by TGF-β

As we have constructed a highly efficient and sensitive replicon system using a luciferase reporter and curedMH14 cells, we used this system to screen anti-HCV compounds. Treatment for 3 days with IFN-α, IL-1β, or cyclosporin A reduced the observed luciferase activities to 3.8%, 9.5%, or 3.4% of control levels, respectively (Fig. 2A). As all three treatments have been reported to repress HCV replicon (Blight et al., 2000; Watashi et al., 2003; Zhu and Liu, 2003), the system is an effective method to screen for potential anti-HCV drugs. We also observed the suppressive effect of TGF-β on luciferase activity (Fig. 2A). While treatment with 2 ng/ml TGF-β (Fig. 2B, open circle) for 36 h had little effect on luciferase activity, enzymatic activity decreased to 11%, 12%, 10% that of the mock-treated cells (black circle) at 48, 60, and 72 h, respectively. To examine